

Title: Advances in Sensitivity and Pulse Detection with Rydberg-Atom Electrometry

Speakers: Stephanie Bohaichuk

Collection: Cold Atom Molecule Interactions (CATMIN)

Date: July 15, 2022 - 1:50 PM

URL: <https://pirsa.org/22070017>

Abstract: The strong interaction of optically excited Rydberg atoms with external fields has made them promising for the detection of radio frequency (RF) electric fields with high sensitivity. Such Rydberg-atom based sensors offer advantages over conventional metal antennas in RF transparency and self-calibration, enabled by all-dielectric construction and extremely well-known atomic properties. In this talk, we describe recent advances in the sensing of low amplitude RF electric fields and the timing of sub-microsecond RF pulses using room temperature Cesium vapour cells. We examine their transient response to RF pulses with durations ranging from 10 μ s to 50 ns, identifying the dependence of atomic time scales on Rabi frequencies and dephasing mechanisms. We present a method for extracting the arrival time of RF pulses in a typical two-photon setup using a matched filter tailored to the atomic response, achieving a field sensitivity down to $\sim 240 \text{ nV cm}^{-1} \text{ Hz}^{-1/2}$ and a timing precision of $\sim 30 \text{ ns}$. On the other hand, practical operation at room temperature results in the self-calibration and sensitivity of this setup being limited by residual Doppler broadening. We therefore develop a novel sub-Doppler approach using a colinear three-photon scheme, which extends the self-calibrated Autler-Townes regime to significantly weaker RF electric fields. With this setup, we achieve a $\sim 200 \text{ kHz}$ spectral linewidth of the Rydberg atoms' electromagnetically induced transparency within a room temperature vapour cell. The results demonstrate the potential of Rydberg atombased sensors for use in test and measurement, communications, and radar applications. "



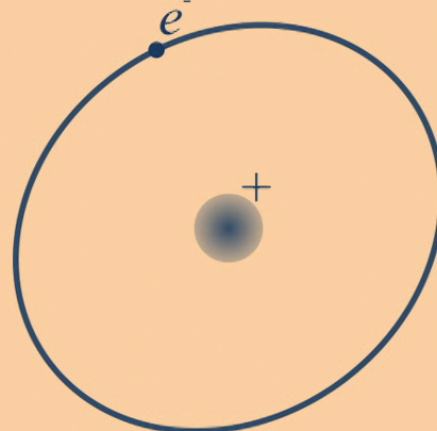
Advances in Sensitivity and Pulse Detection with Rydberg-Atom Electrometry

S. Bohaichuk, F. Ripka, D. Booth, C. Liu, M. Schmidt,
K. Nickerson, H. Tai, H. Kübler, J. Shaffer

CATMIN 2022

Rydberg Atom Electrometry

- Rydberg states of alkalis (Cs, Rb) with high n have exaggerated properties
 - Strong dipole moments μ that are known precisely
- High sensitivity to radio frequency (RF) electric fields
- Compact sensors of room temperature vapour



Typical Cs Transition Dipole Moments

$$\mu (6S_{1/2} \leftrightarrow 6P_{3/2}) = 4.48 \text{ ea}_0$$

$$\mu (5S_{1/2} \leftrightarrow 5P_{3/2}) = 6294 \text{ ea}_0$$

$$\mu (4D_{5/2} \leftrightarrow 4P_{3/2}) = 980 \text{ ea}_0$$

Quantity	Symbol	Scaling
Radius	$\langle r \rangle$	n^2
Transition Dipole	$\langle nl er nl' \rangle$	n^2
Polarizability	α	n^7
Dipole - Dipole Interaction	C_3	n^4

Journal of Physics B **53**, 012002 (2019)

Sensing an Electric Field

Rydberg state Atomic Energy Levels

- Dark state (EIT) created using interaction of several lasers
- Bright state when external RF E-field added (Autler-Townes splitting)
- Sensitivity to microwave is large because dipole moment is large
- RF to optical transduction for readout via probe absorption changes

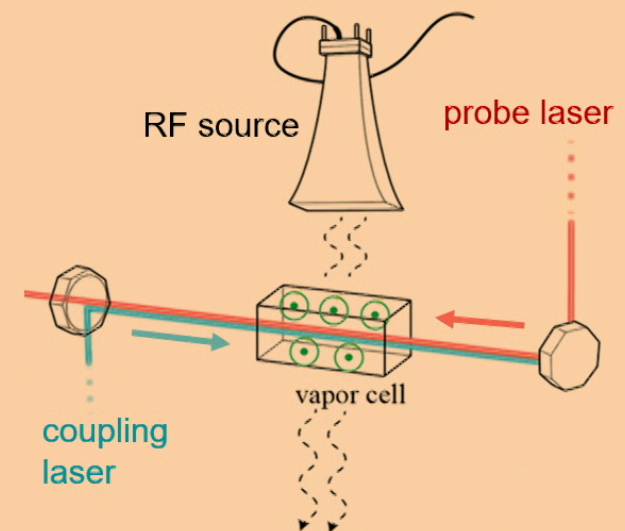
Rydberg state

Excited state

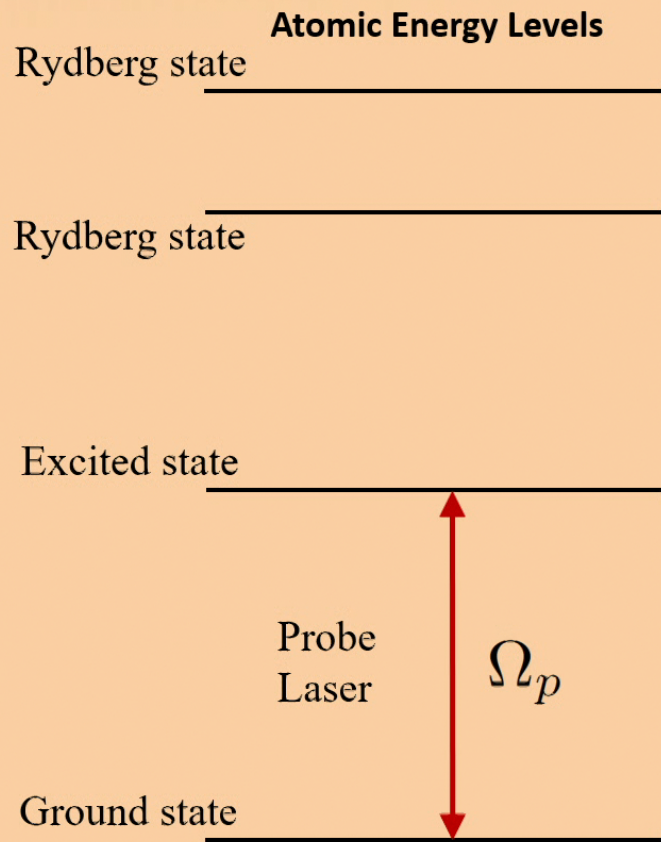
Ground state

Probe
Laser

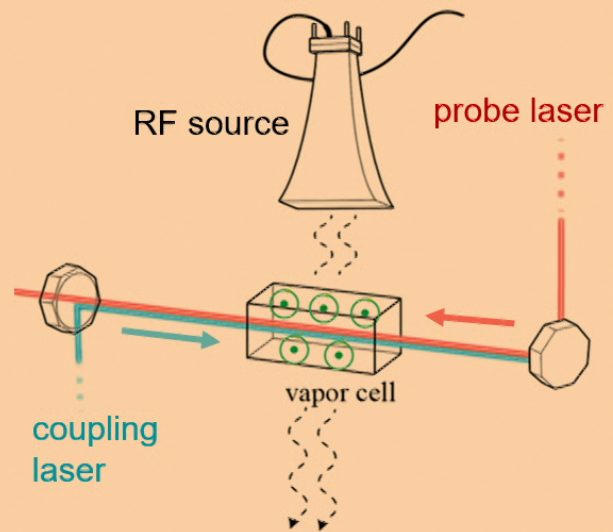
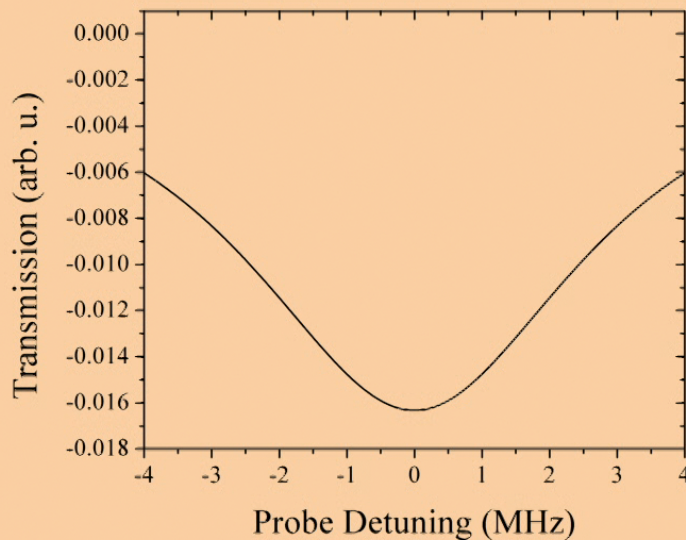
Ω_p



Sensing an Electric Field



- Dark state (EIT) created using interaction of several lasers
- Bright state when external RF E-field added (Autler-Townes splitting)
- Sensitivity to microwave is large because dipole moment is large
- RF to optical transduction for readout via probe absorption changes



S. Bohaichuk

Quantum Valley
Ideas Lab

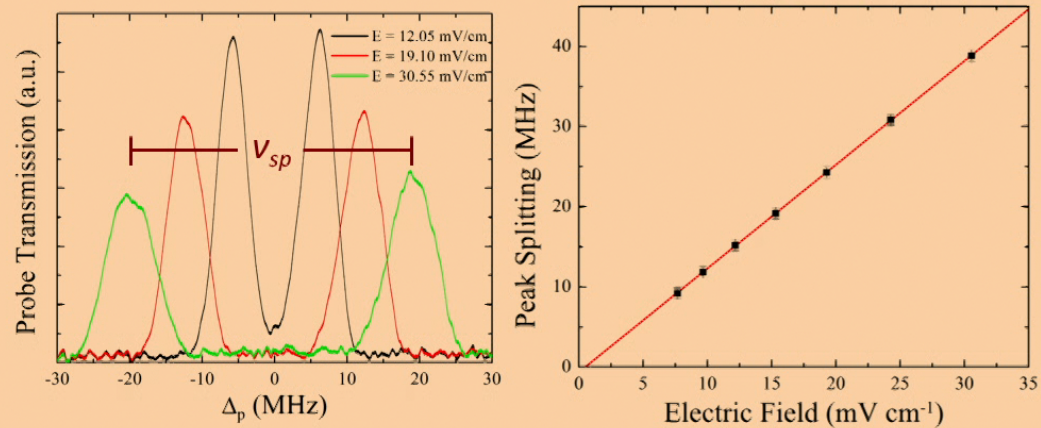
3

Autler-Townes & Amplitude Regimes

- In the Autler-Townes regime (larger amplitude RF E-fields), peaks are split:

$$E_{RF} = \frac{2\pi\hbar\nu_{sp}}{\mu}$$

- Depends only on well-known μ



Autler-Townes & Amplitude Regimes

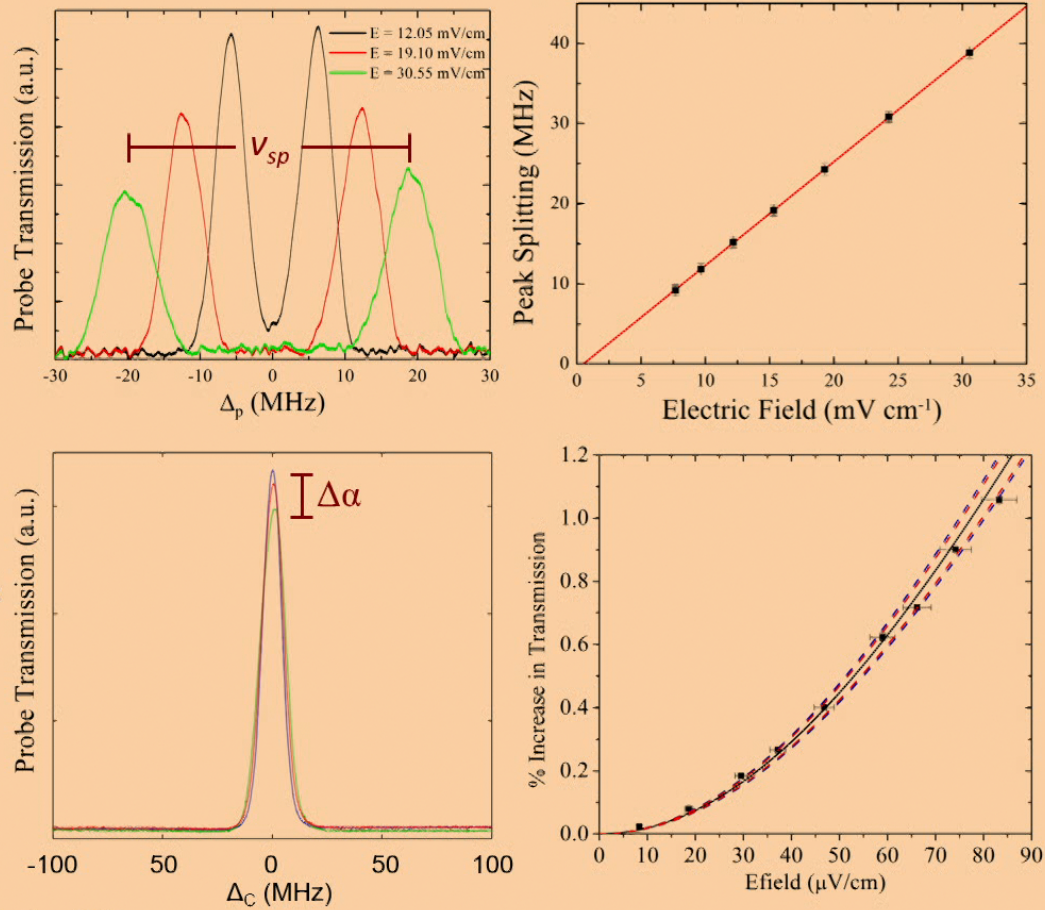
- In the Autler-Townes regime (larger amplitude RF E-fields), peaks are split:

$$E_{RF} = \frac{2\pi\hbar\nu_{sp}}{\mu}$$

- Depends only on well-known μ
- In amplitude regime (weaker amplitude RF E-fields) peak height changes:

$$E_{RF} \sim \frac{\hbar}{\mu} \left[\frac{\sqrt{1 - \lambda_p/\lambda_c} \left((-1 + \lambda_p/\lambda_c)\gamma_2 + \gamma_3 \right) \Omega_C}{2} \Delta\alpha \right]^{1/2}$$

- Depends non-linearly on decay rates (γ), laser conditions (Ω_C) and change in absorption ($\Delta\alpha$)



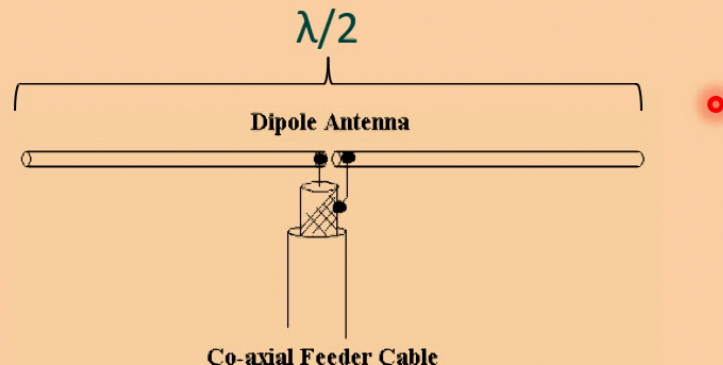
S. Bohaichuk

Quantum Valley
Ideas Lab

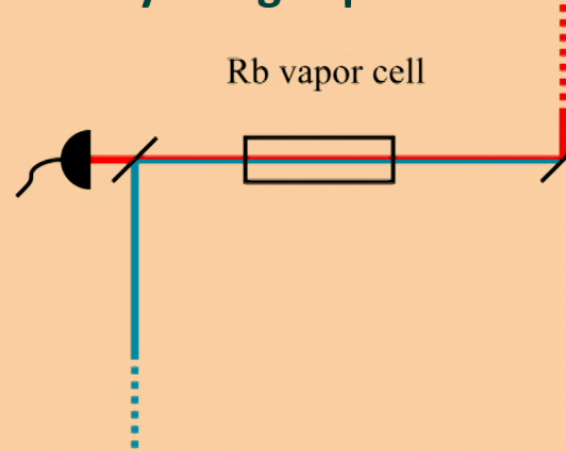
4

Traditional Antennas vs Rydberg Atoms

Traditional Dipole antenna



Rydberg vapour cell

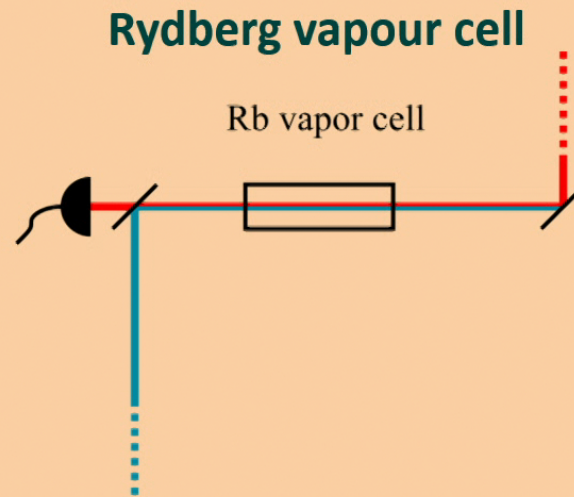


- Electrons moving in a metal
- Electrical readout
- Collection of atoms as the 'antennas'
- Optical readout

Traditional Antennas vs Rydberg Atoms

Advantages

- Self-calibration linked to fundamental constants and atomic properties
- Electromagnetically transparent (dielectric)
- Stability, reproducibility
- Sub-wavelength with imaging possible
- Broad carrier bandwidth: MHz – THz



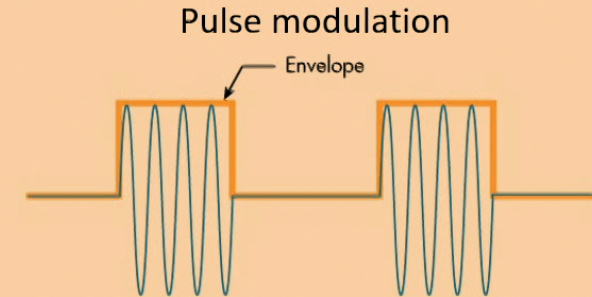
- Collection of atoms as the 'antennas'
- Optical readout

Outline

1. What are atomic limits on temporal resolution?

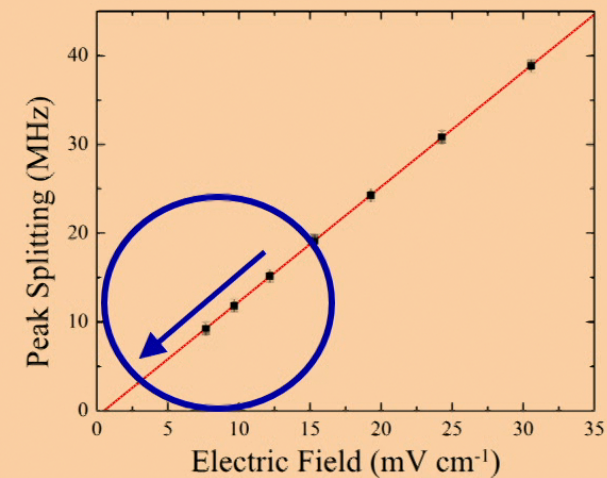
- Transit time, collisions, ions? 
- Pulse modulated RF
- Applications in radar & communications

S. Bohaichuk, arXiv:2203.01733 (2022).



2. How can we improve sensitivity?

- Weakest field detectable in shortest time
- Extension of Autler-Townes regime to lower fields



S. Bohaichuk

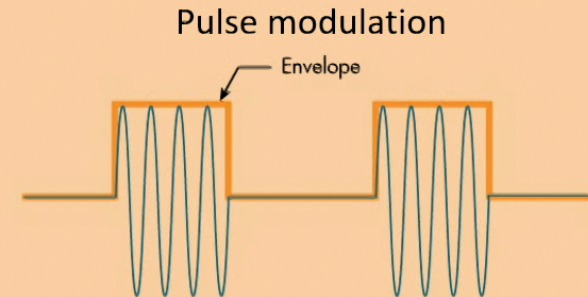
Quantum Valley
Ideas Lab

Outline

1. What are atomic limits on temporal resolution?

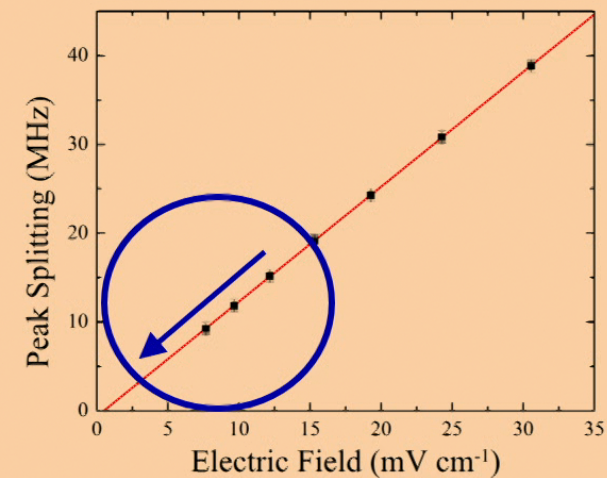
- Transit time, collisions, ions? 
- Pulse modulated RF
- Applications in radar & communications

S. Bohaichuk, arXiv:2203.01733 (2022).



2. How can we improve sensitivity?

- Weakest field detectable in shortest time
- Extension of Autler-Townes regime to lower fields



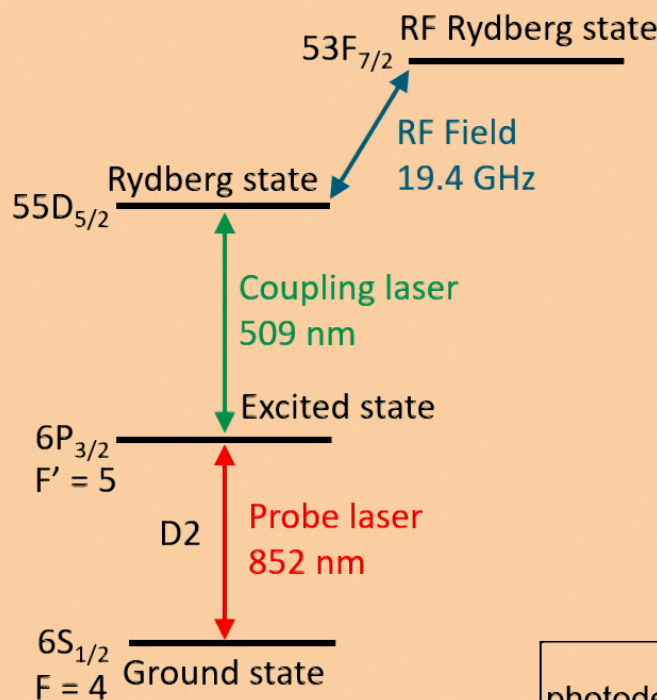
S. Bohaichuk

Quantum Valley
Ideas Lab

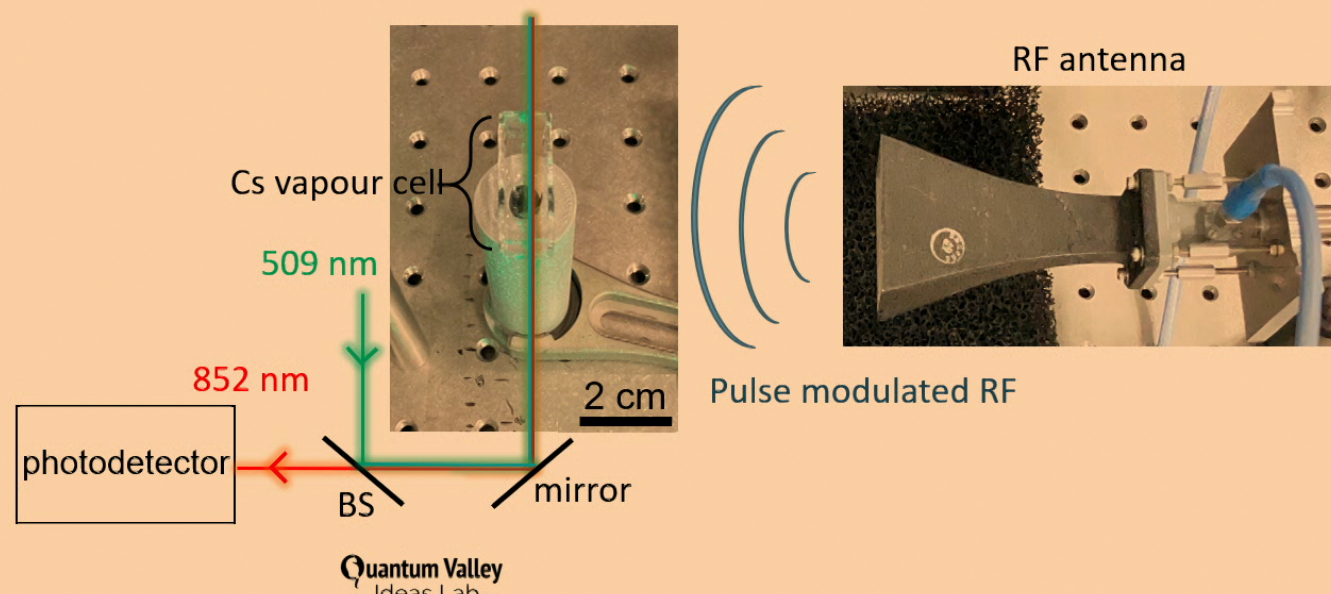
7

2-Photon Scheme for RF Sensing

Cs Atomic Energy Levels

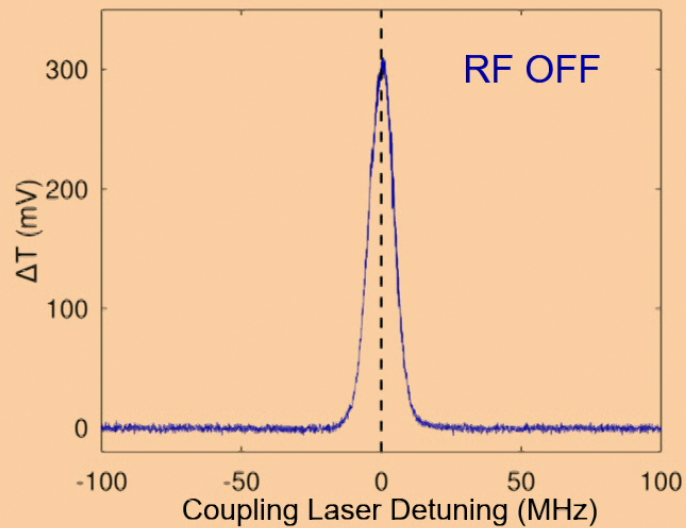
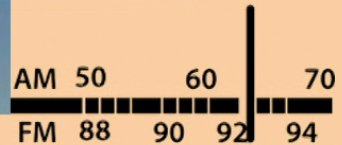


- Counterpropagating 852 nm and 509 nm diode lasers
- Both lasers locked on resonance referenced to ultra-stable cavity
- Pulse modulated RF field induces change in probe transmission



Pulse-Modulated RF Detection

- Sub-microsecond pulses typical in radar & communications
- Need to understand limits to atomic response time
- Goal to precisely detect weak RF pulse arrival time



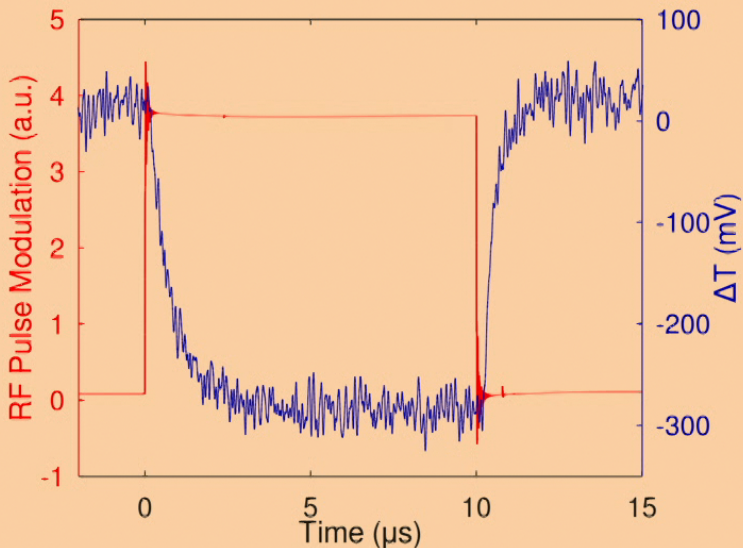
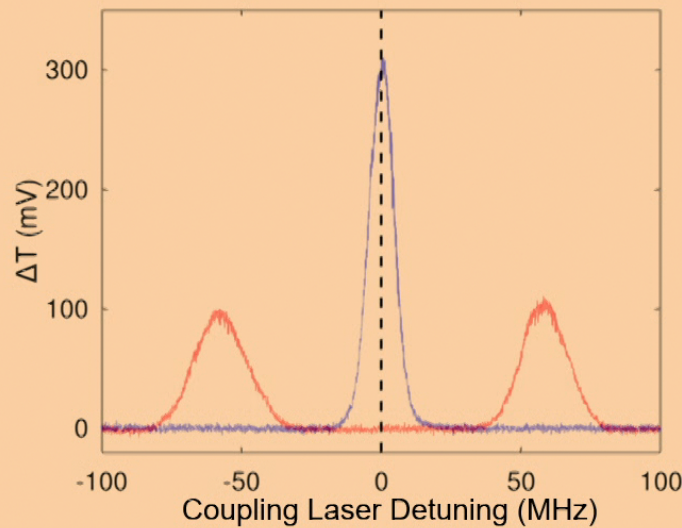
S. Bohaichuk

Quantum Valley
Ideas Lab

9

Pulse-Modulated RF Detection

- Sub-microsecond pulses typical in radar & communications
- Need to understand limits to atomic response time
- Goal to precisely detect weak RF pulse arrival time

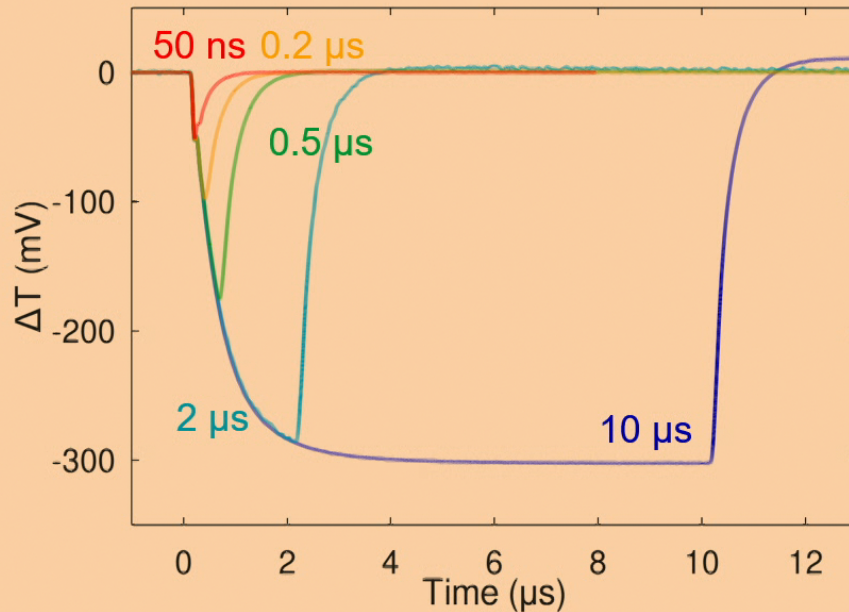
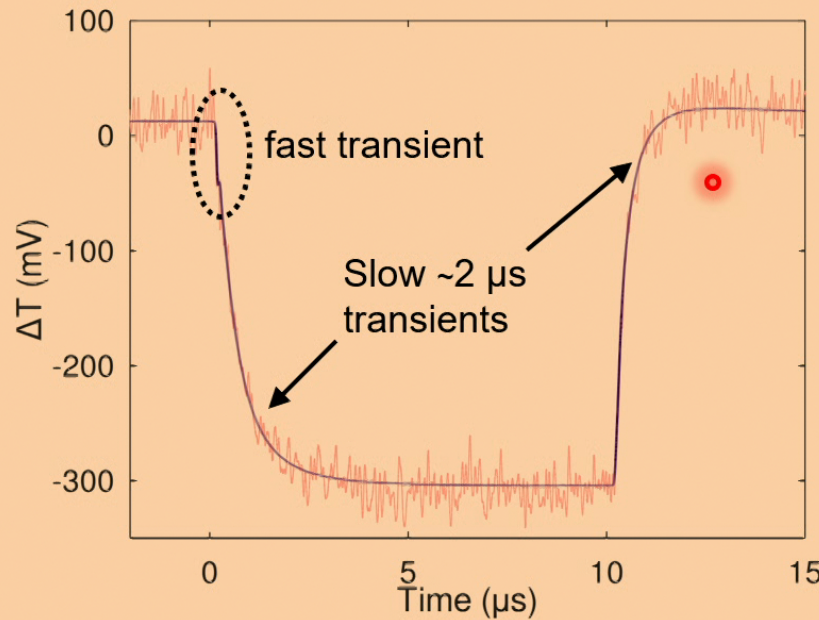


S. Bohaichuk

Quantum Valley
Ideas Lab

9

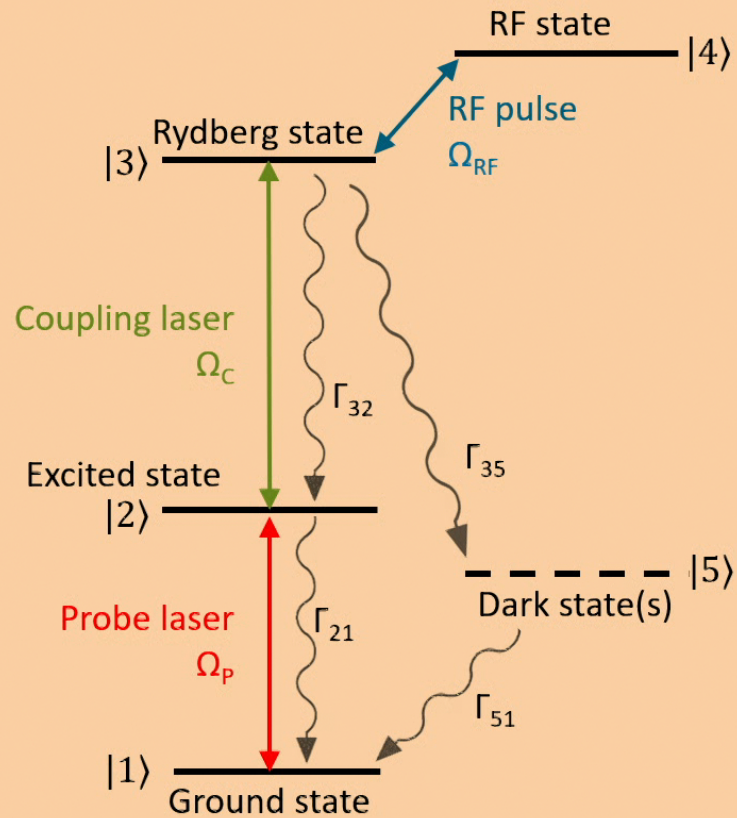
Transient Atomic Response



- Initial rapid drop in transmission lasting <50 ns, dependent on probe laser power
- Slow transient to steady state takes several μ s
- Slow response limits total pulse depth when shorter RF pulses are used

$$\begin{aligned}\Omega_P &= 2\pi \times 3.5 \text{ MHz} \\ \Omega_C &= 2\pi \times 2.1 \text{ MHz}\end{aligned}$$

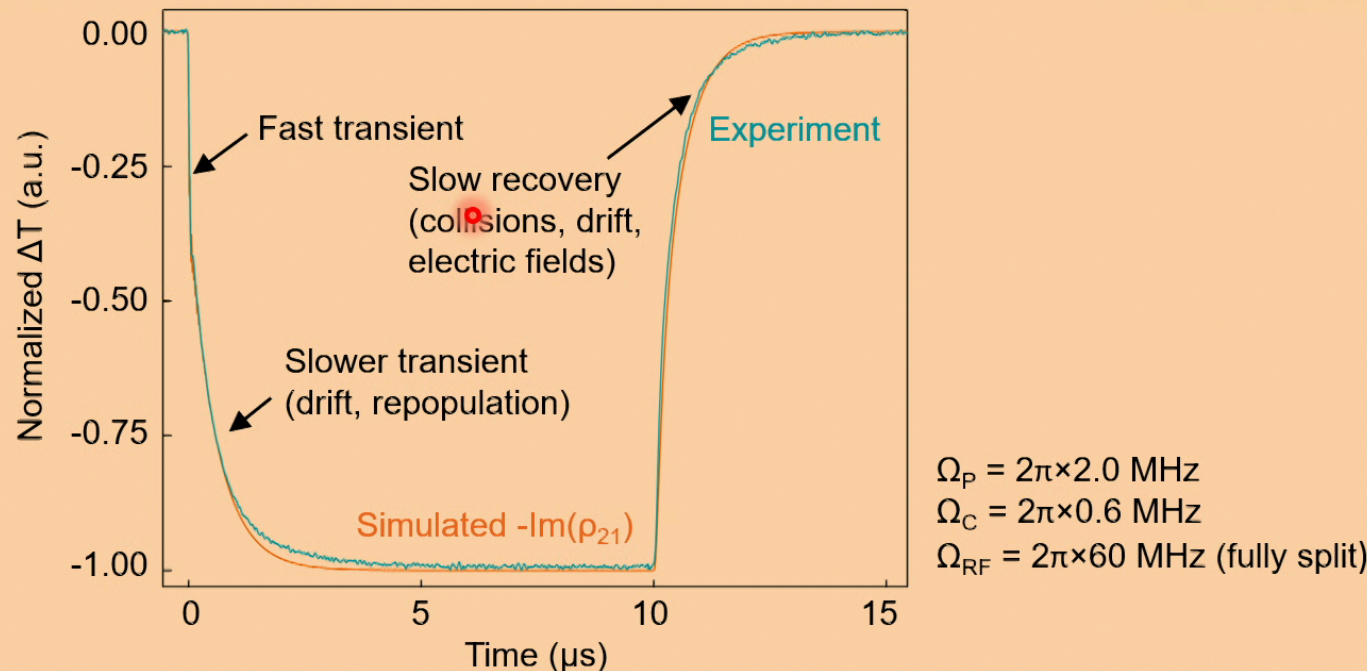
Density Matrix Modeling



$$\dot{\rho} = \frac{i}{\hbar} [\rho, H] + \mathcal{L}(\rho)$$

- Time-varying Hamiltonian with pulsed RF Rabi frequency
- Rates (Γ 's) represent decays & decoherences for these experimental conditions:
- Known decays: $\Gamma_{21} = 2\pi \times 5.2 \text{ MHz}$, $\Gamma_{32} = 2\pi \times 10.4 \text{ kHz}$
- Transit time: $\Gamma_{31} = \Gamma_{41} = \Gamma_{51} = 2\pi \times 275 \text{ kHz}$
- Dark state generation: $\Gamma_{35} = 2\pi \times 10 - 800 \text{ kHz}$ which captures:
 - State-changing Rydberg-Rydberg collisions
 - Ion generation via collisions & blackbody radiation

Atomic Time Scales



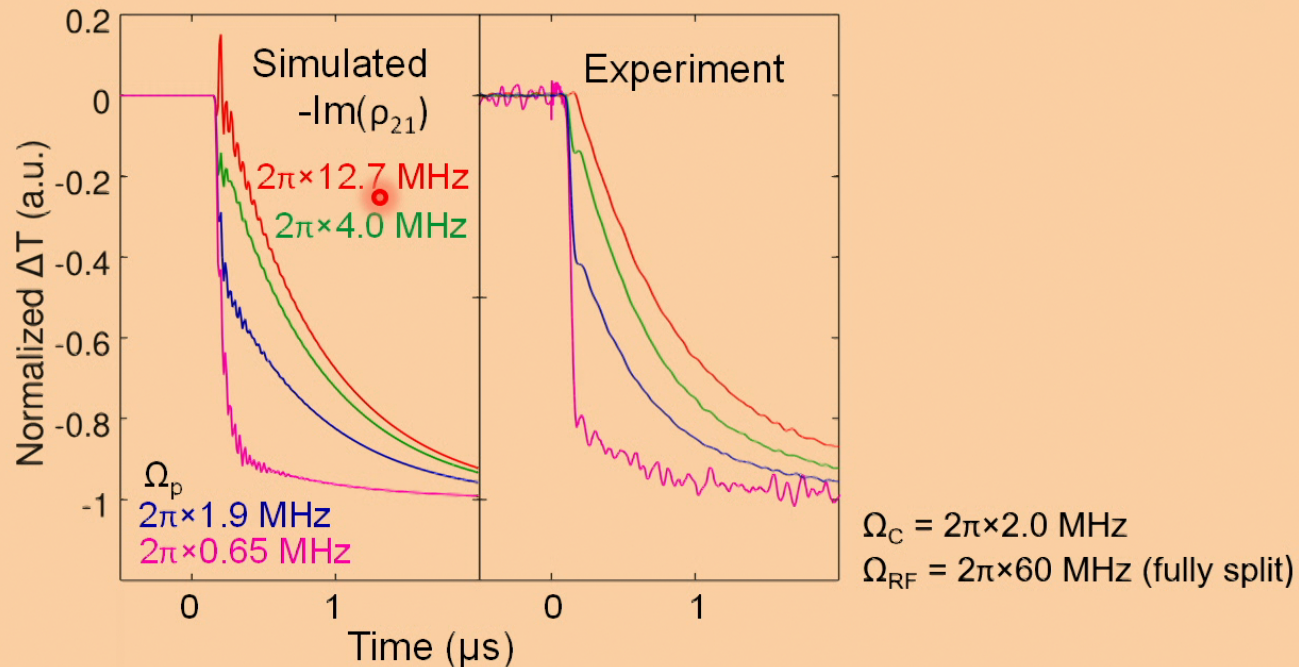
1. Fast Transient – rapid two-level (D2 line) re-equilibration
2. Slow Transient – removal of Rydberg & dark atoms set by transit time
3. Slow Recovery – regeneration of Rydberg & dark atoms set by collisions, electric fields, & transit time as coupling laser restored to initial conditions

S. Bohaichuk

Quantum Valley
Ideas Lab

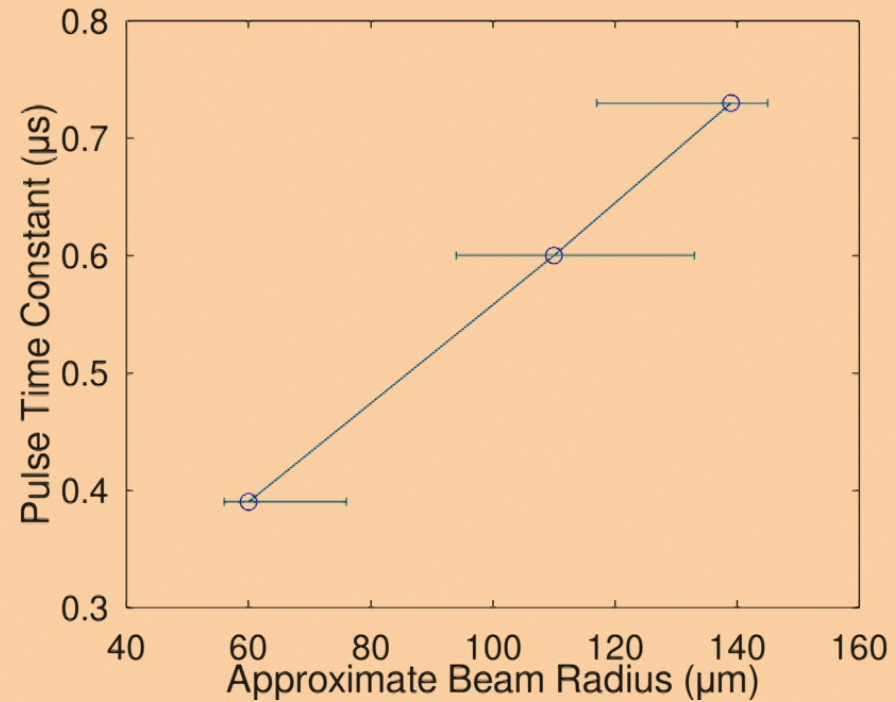
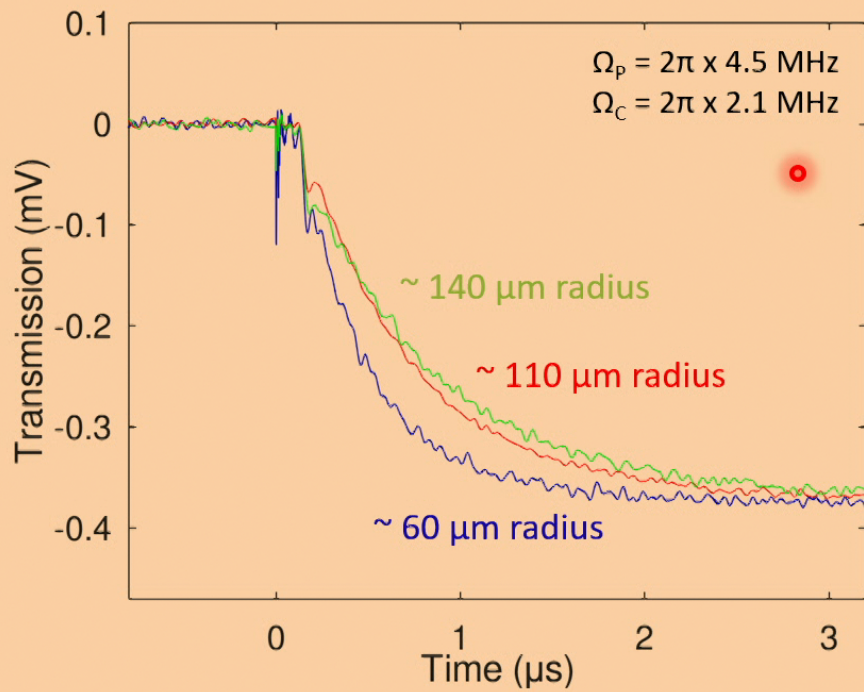
12

Atomic Time Scales – Fast Transient



- Deeper initial transient is present at lower probe laser Rabi frequencies
- Improves detection of short pulses

Atomic Time Scales – Slower Transient



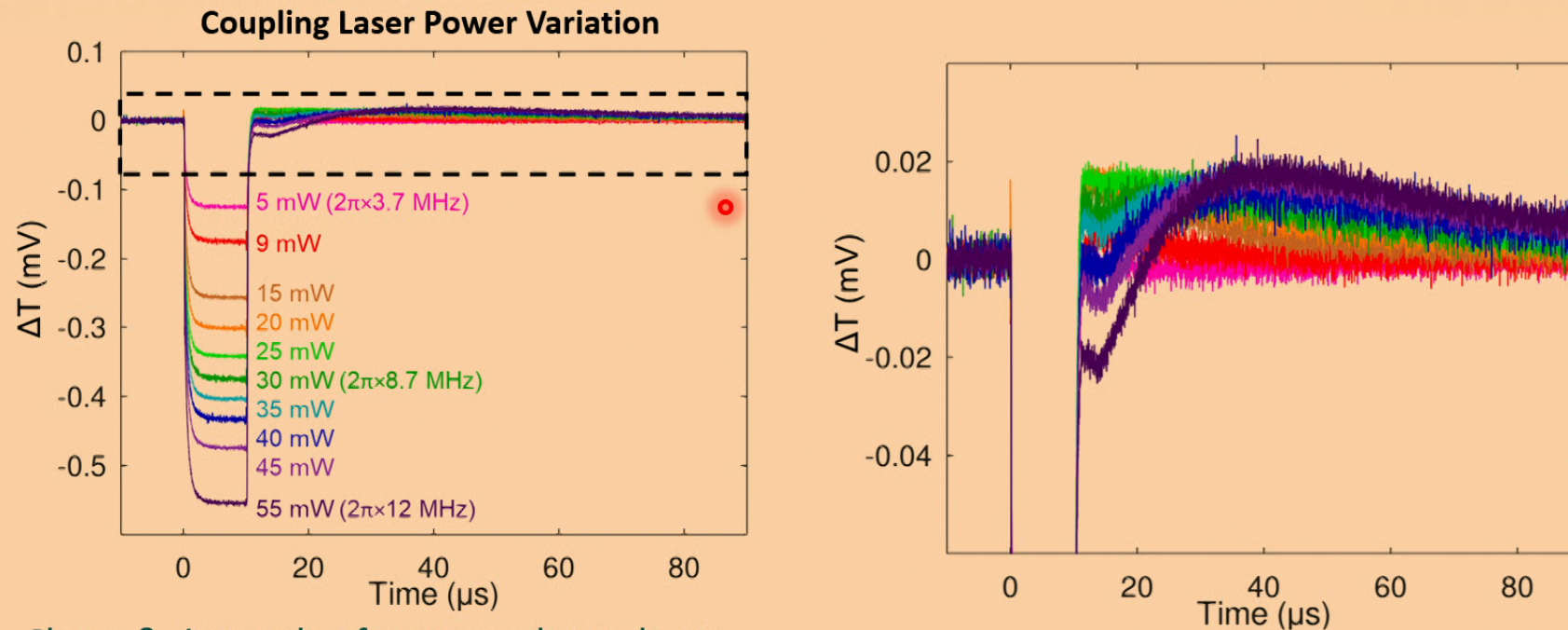
- Atomic response slows as increase laser beam size since atoms linger in optical system
- Overall pulse response time scale limited by transit time

S. Bohaichuk

Quantum Valley
Ideas Lab

14

Atomic Time Scales – Recovery



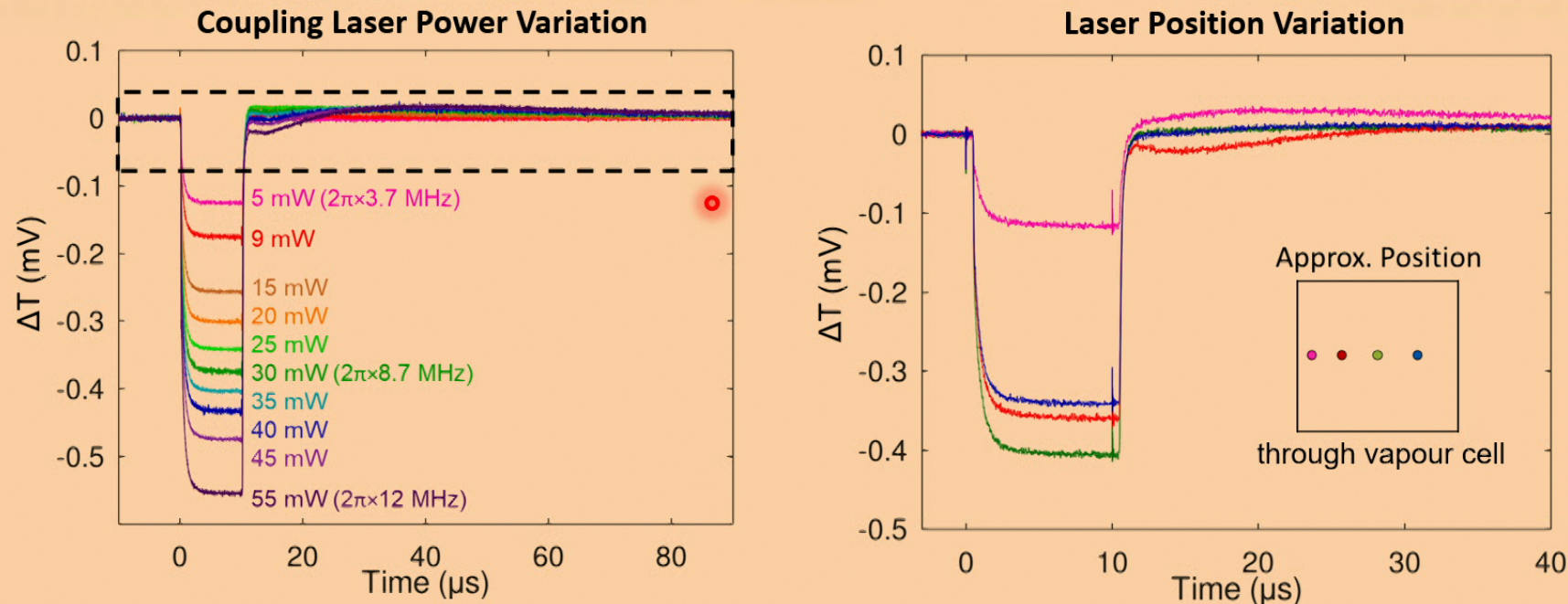
- Shape & timescale of recovery depends on:
 - Excited-Rydberg transition choice (which states)
 - Coupling laser power & detuning
 - Position of beams within vapour cell
- Result of collisional and electric field effects at higher Rydberg populations, partly modeled with dark state

S. Bohaichuk

Quantum Valley
Ideas Lab

15

Atomic Time Scales – Recovery



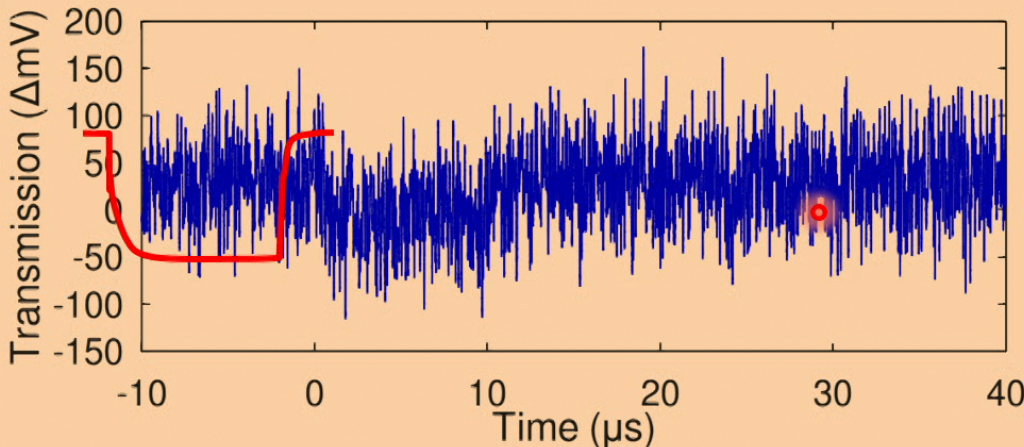
- Shape & timescale of recovery depends on:
 - Excited-Rydberg transition choice (which states)
 - Coupling laser power & detuning
 - Position of beams within vapour cell
- Result of collisional and electric field effects at higher Rydberg populations, partly modeled with dark state

S. Bohaichuk

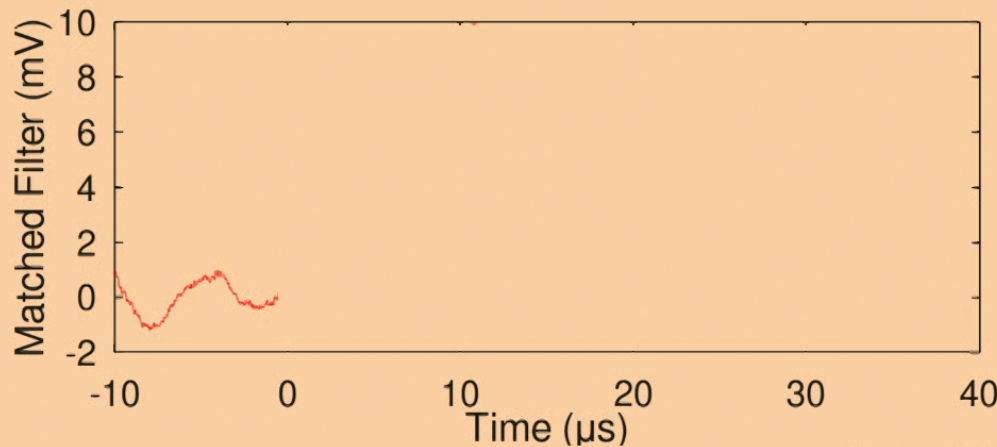
Quantum Valley
Ideas Lab

15

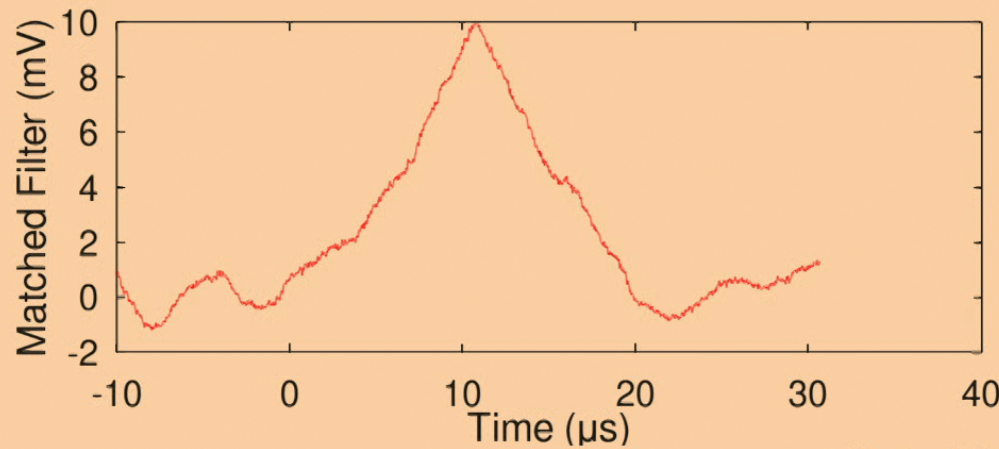
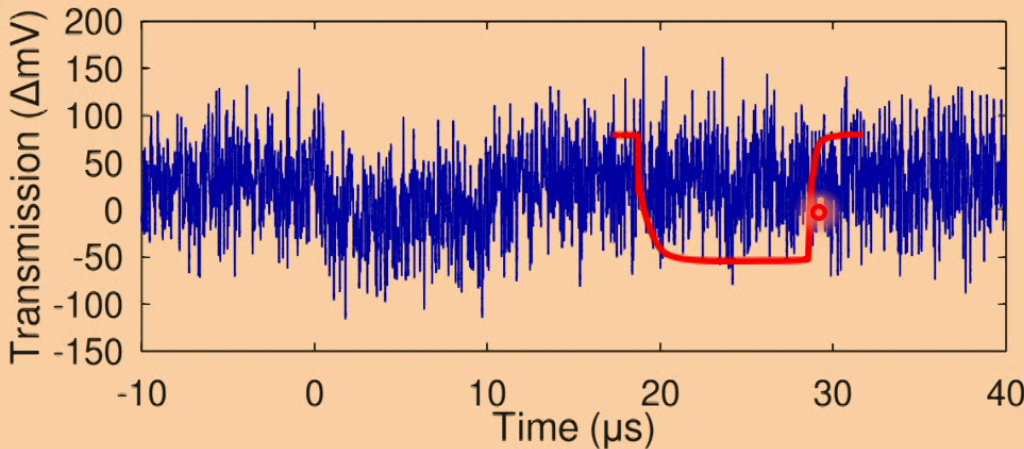
Pulse Detection: Matched Filtering



- Used in communications to detect weak signals buried in noise
- Extracts pulse end time by maximizing correlation with a known pulse template
- Template can be simulated or an averaged experimental pulse
- Implemented in real-time with an FPGA

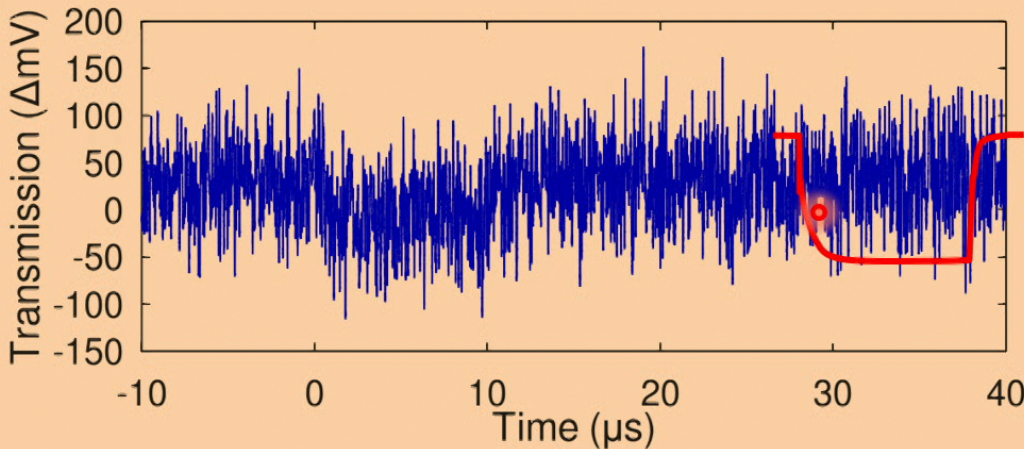


Pulse Detection: Matched Filtering

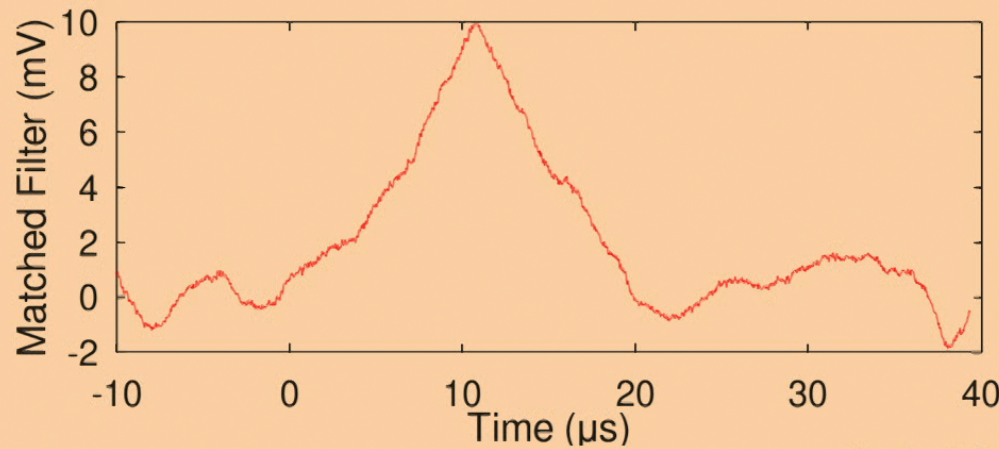


- Used in communications to detect weak signals buried in noise
- Extracts pulse end time by maximizing correlation with a known pulse template
- Template can be simulated or an averaged experimental pulse
- Implemented in real-time with an FPGA

Pulse Detection: Matched Filtering

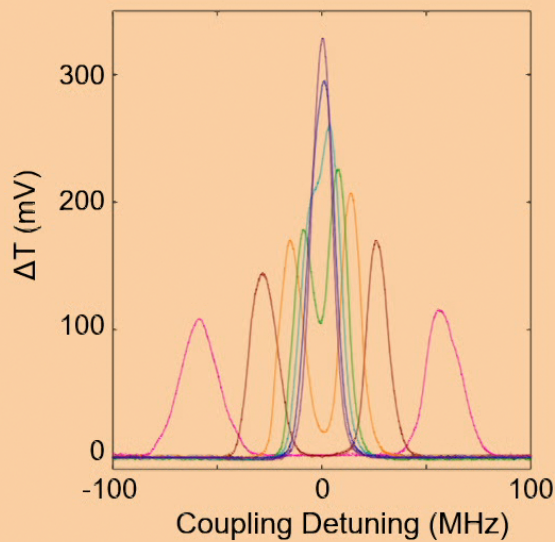


- Used in communications to detect weak signals buried in noise
- Extracts pulse end time by maximizing correlation with a known pulse template
- Template can be simulated or an averaged experimental pulse
- Implemented in real-time with an FPGA

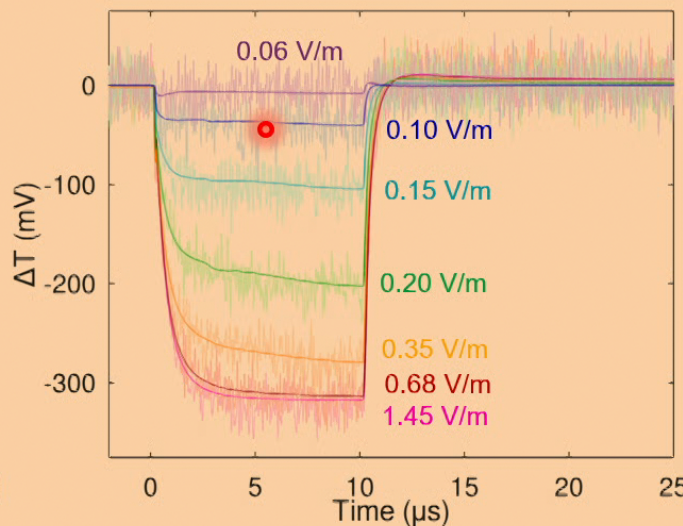


Filtered Individual Pulses

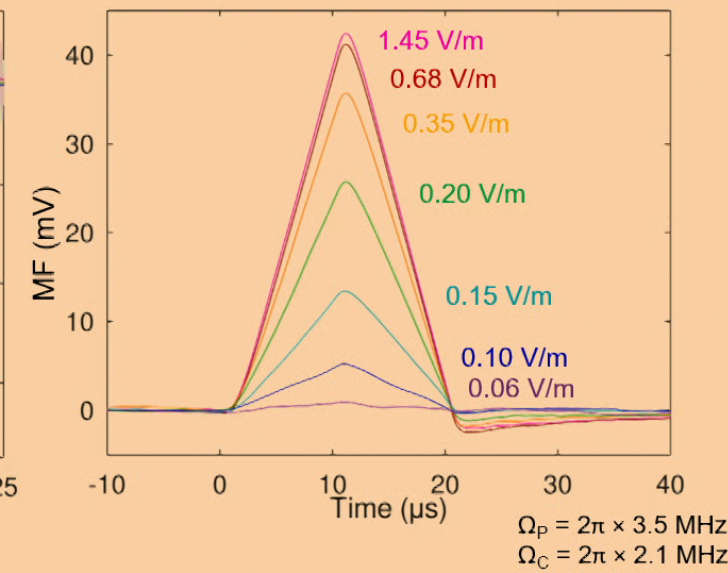
Continuous Wave RF Response



Pulsed RF Optical Response

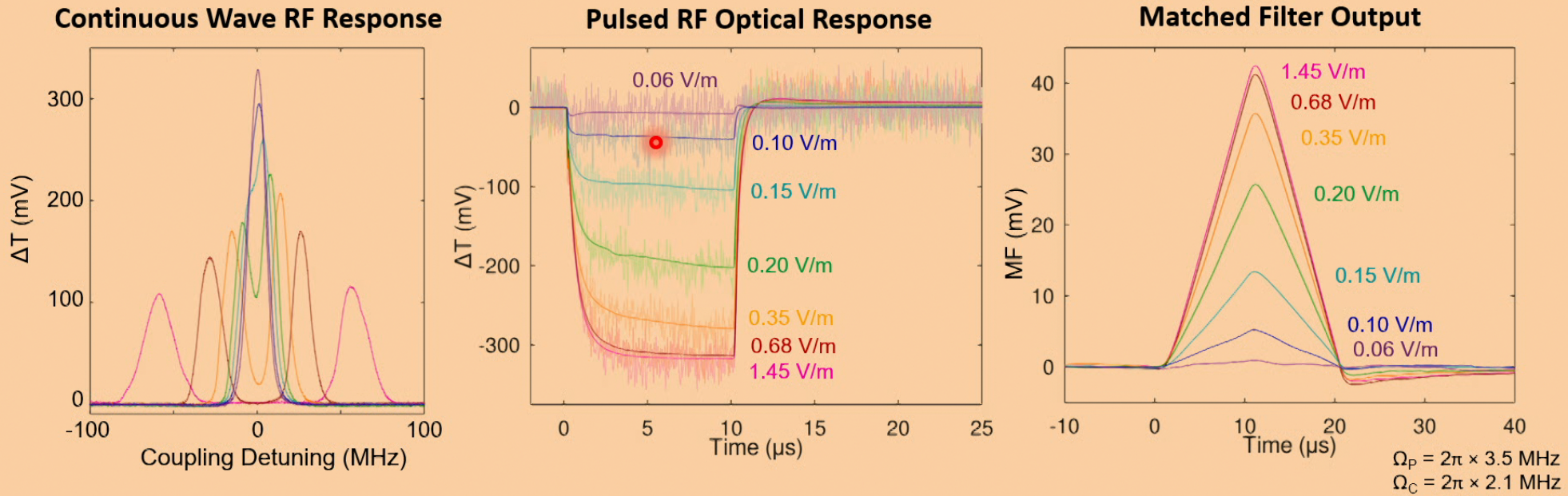


Matched Filter Output



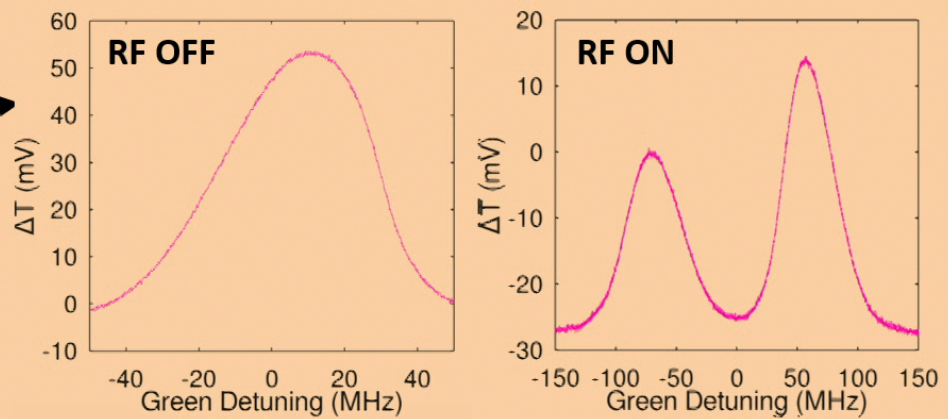
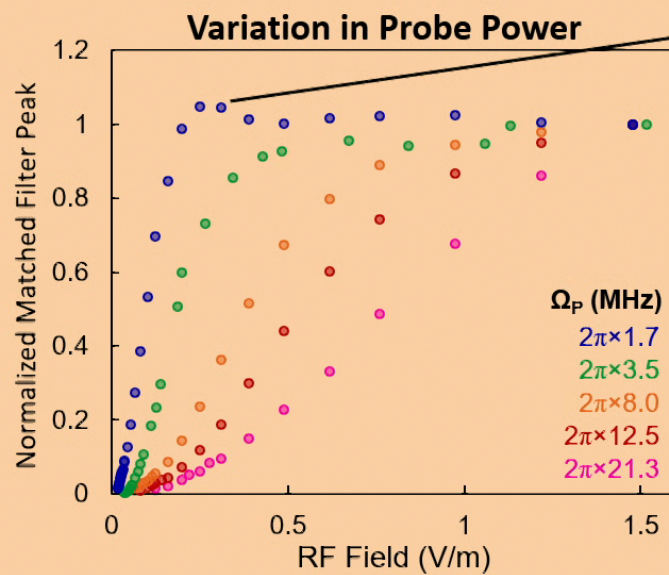
- RF field strength nonlinearly changes pulse depth in absorption regime
- Pulse depth saturates in Autler-Townes regime
- Matched filter applied to single pulses greatly improve signal-to-noise (SNR) & extracts timing

Filtered Individual Pulses



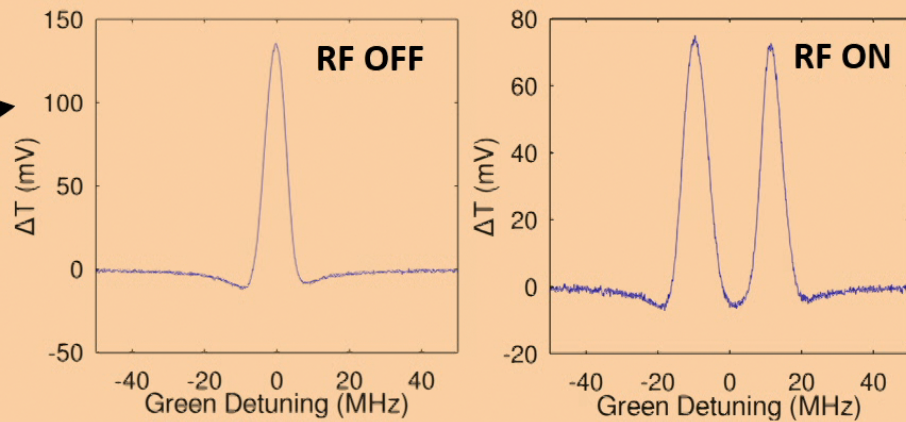
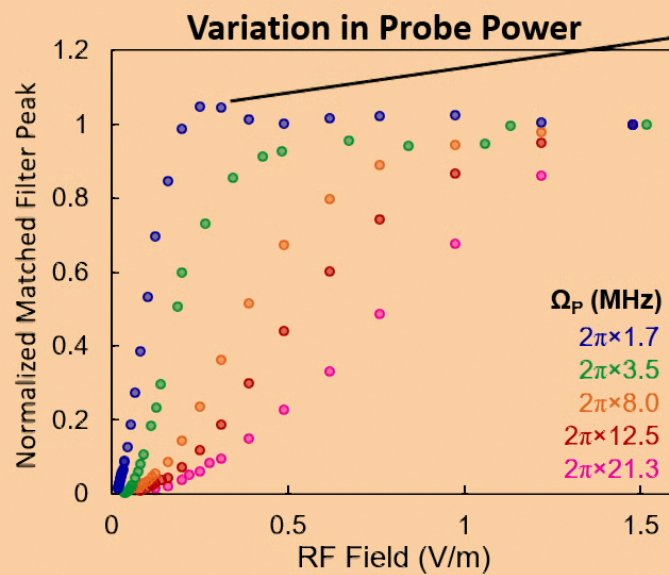
- RF field strength nonlinearly changes pulse depth in absorption regime
- Pulse depth saturates in Autler-Townes regime
- Matched filter applied to single pulses greatly improve signal-to-noise (SNR) & extracts timing

Choice of Laser Conditions



- Lower probe power improves SNR but cannot distinguish powers of large RF fields

Choice of Laser Conditions



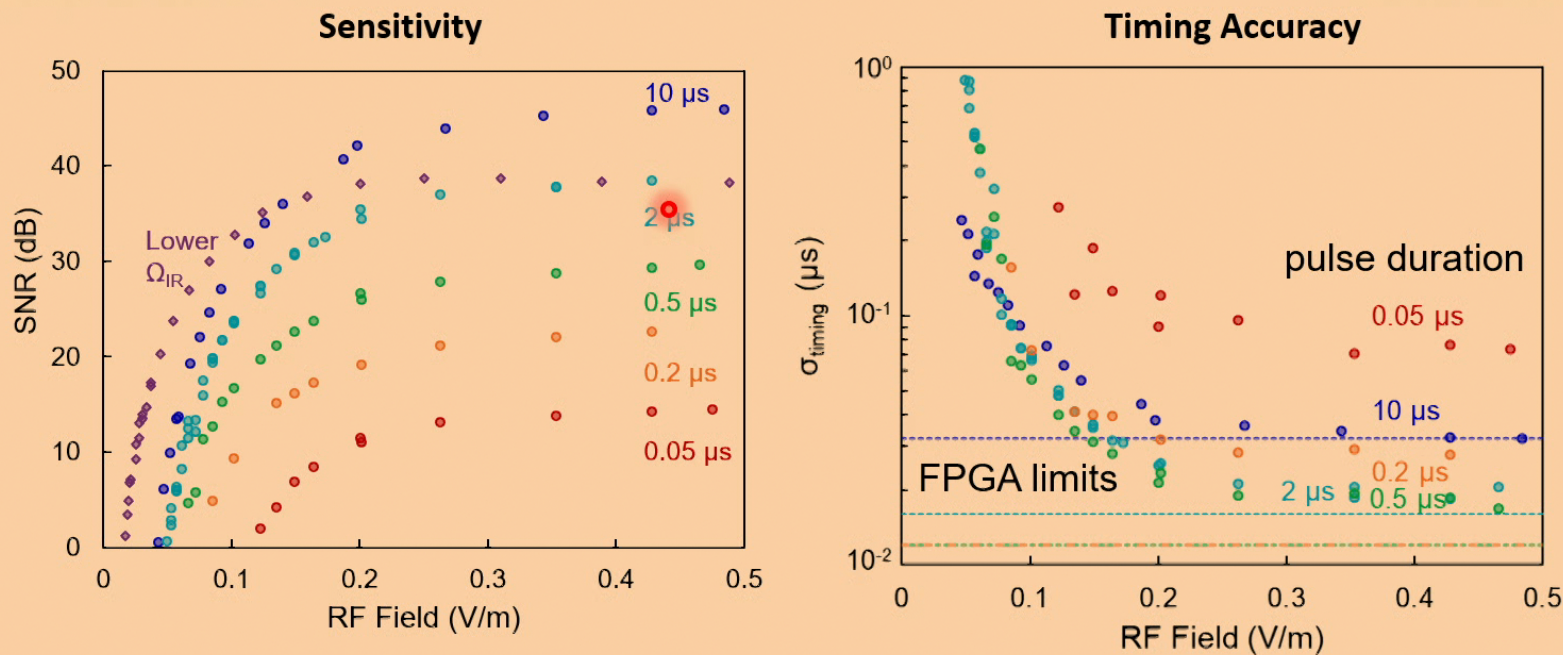
- Lower probe power improves SNR but cannot distinguish powers of large RF fields
- Lower coupling power advantageous until reach noise limits

S. Bohaichuk

Quantum Valley
Ideas Lab

19

Atomic Receiver Performance



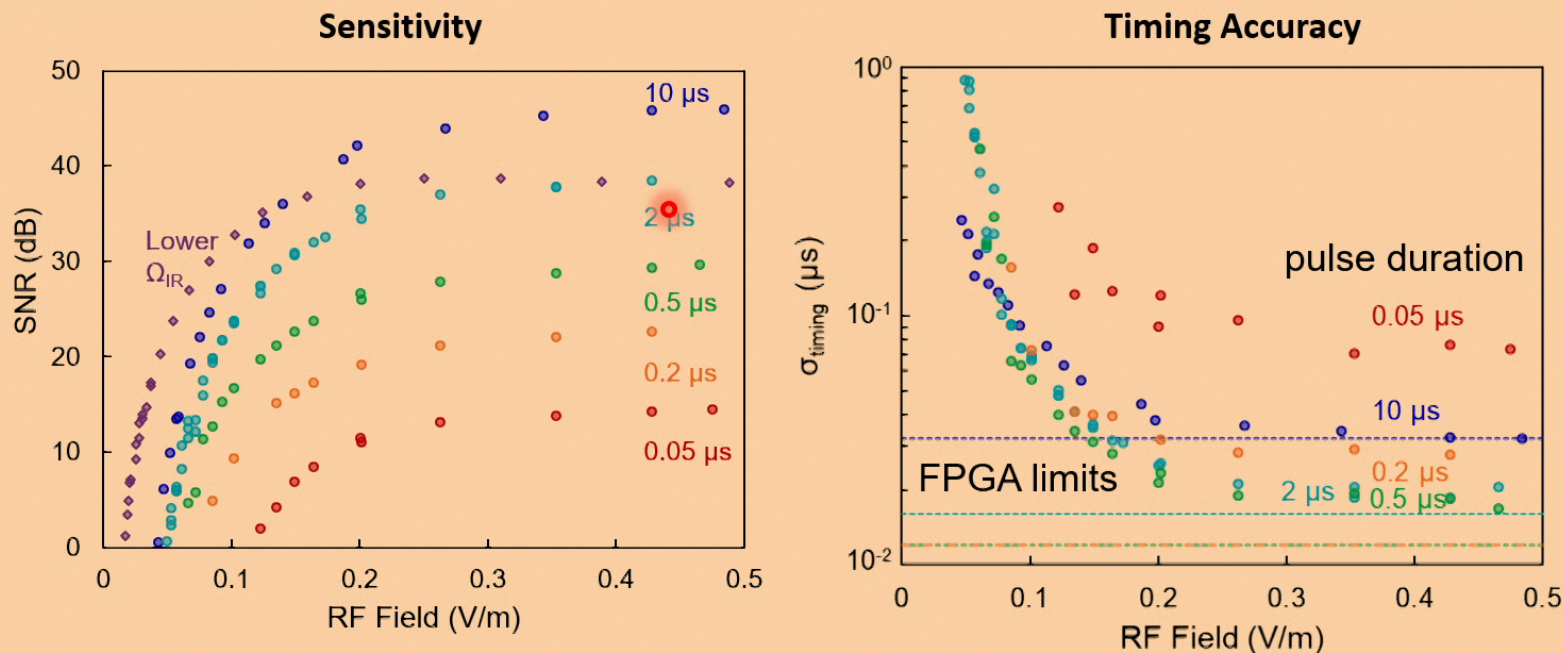
- Sensitivity degrades for pulse durations below the $\sim 2 \mu\text{s}$ atomic response
- Minimum detectable field $\sim 170 \mu\text{V}/\text{cm}$ with sensitivity $\sim 240 \text{nV cm}^{-1} \text{Hz}^{-1/2}$
- Timing resolution can be $< 30 \text{ ns}$ but degrades at weak RF E-fields

S. Bohaichuk

Quantum Valley
Ideas Lab

20

Atomic Receiver Performance



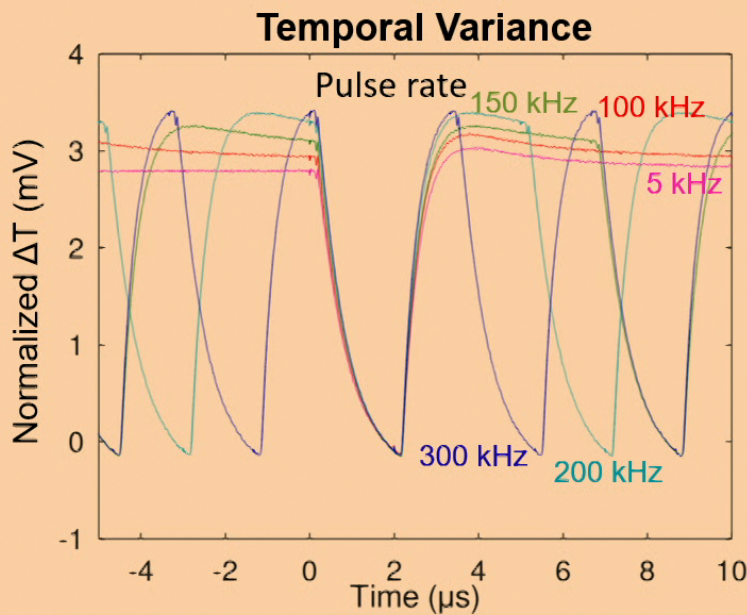
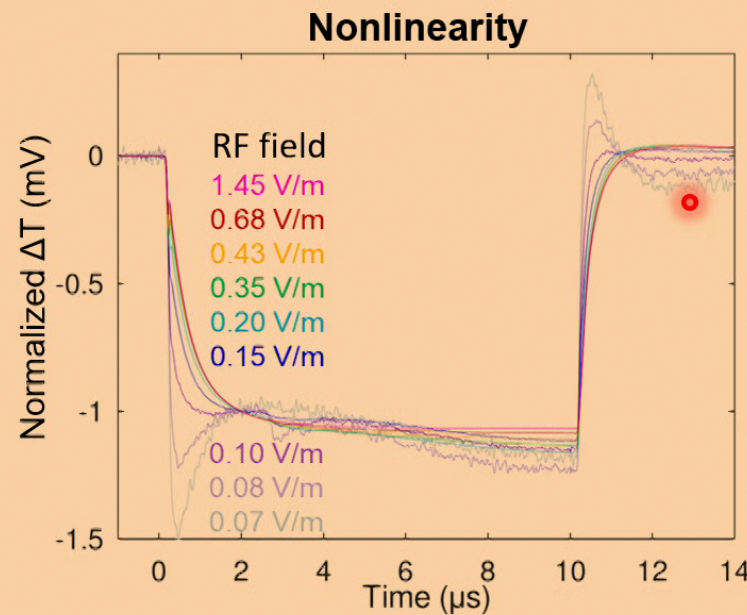
- Sensitivity degrades for pulse durations below the $\sim 2 \mu\text{s}$ atomic response
- Minimum detectable field $\sim 170 \mu\text{V}/\text{cm}$ with sensitivity $\sim 240 \text{nV cm}^{-1} \text{Hz}^{-1/2}$
- Timing resolution can be $< 30 \text{ ns}$ but degrades at weak RF E-fields

S. Bohaichuk

Quantum Valley
Ideas Lab

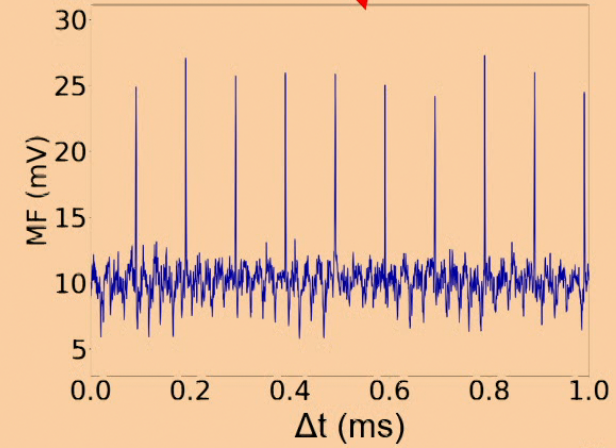
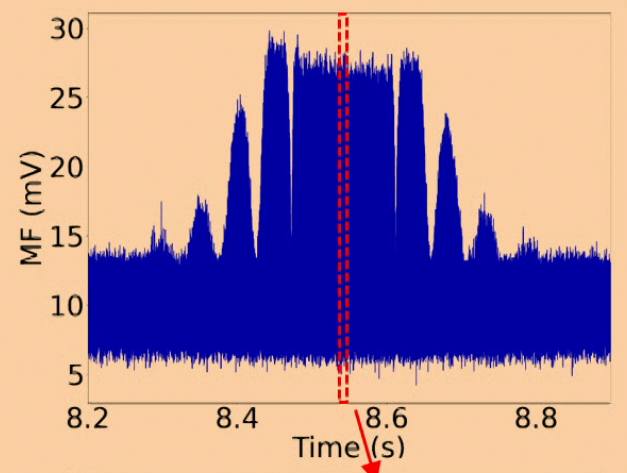
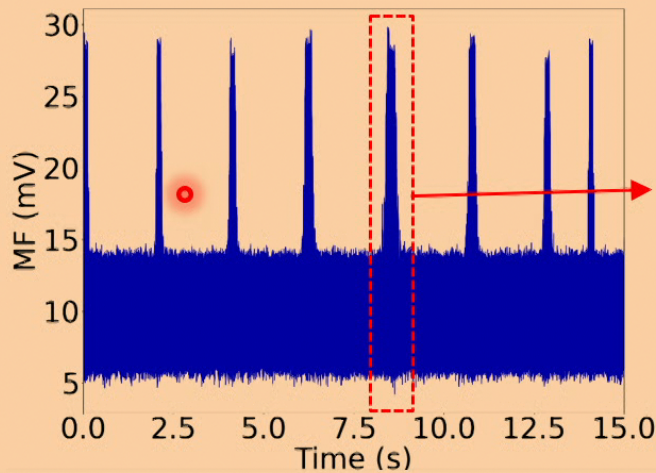
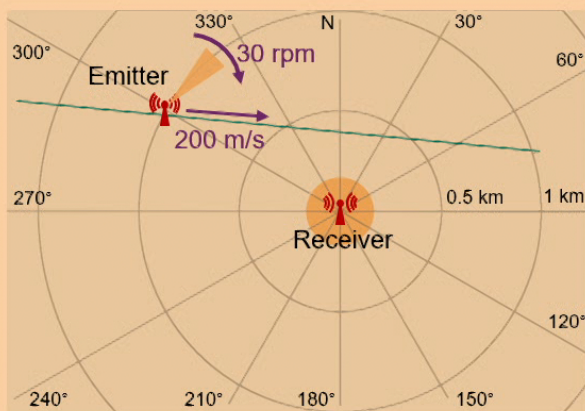
20

Matched Filter Considerations



- Pulse shape changes slightly in the amplitude regime at edges
- Pulse depth and recovery depend slightly on pulse rate relative to slow electric field effects
- Matched filter still functions but extracted pulse timing shifted slightly

Application: Radar Detection

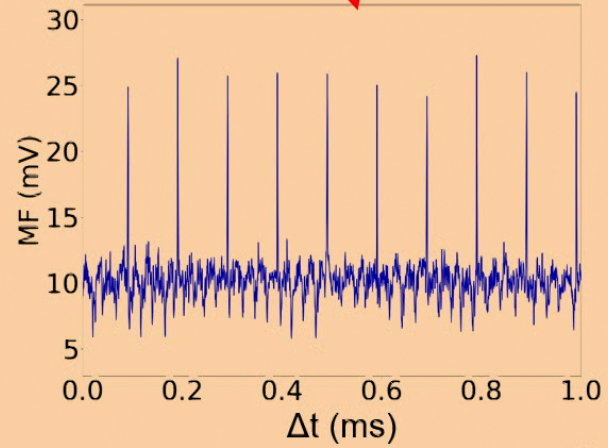
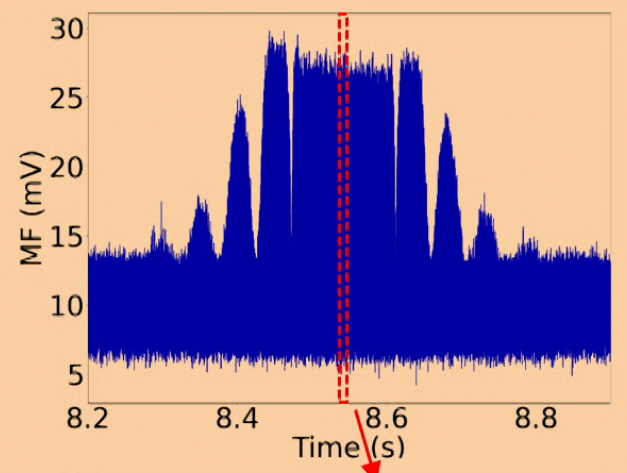
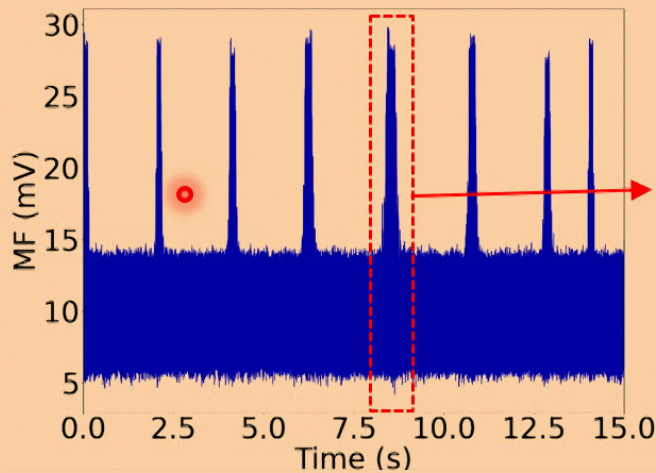
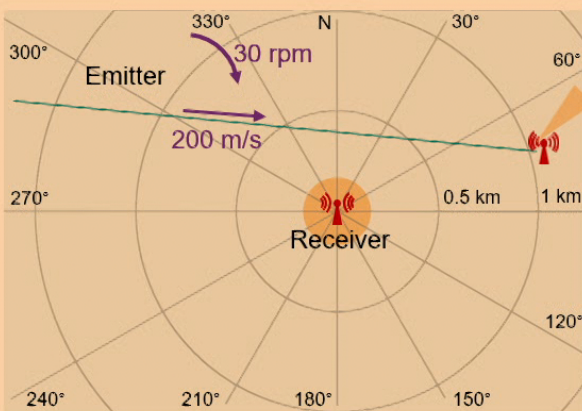


- Experimental radar detected from simulated spinning aircraft emitter
- Captures side lobes of emitter pattern, but central lobe saturates
- Timing resolution of 30 ns corresponds to 9 m spatial resolution

S. Bohaichuk

Quantum Valley
Ideas Lab

Application: Radar Detection



- Experimental radar detected from simulated spinning aircraft emitter
- Captures side lobes of emitter pattern, but central lobe saturates
- Timing resolution of 30 ns corresponds to 9 m spatial resolution

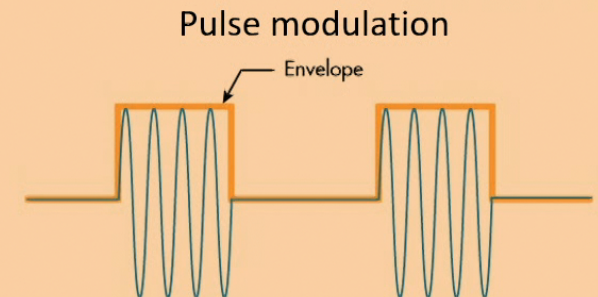
S. Bohaichuk

Quantum Valley
Ideas Lab

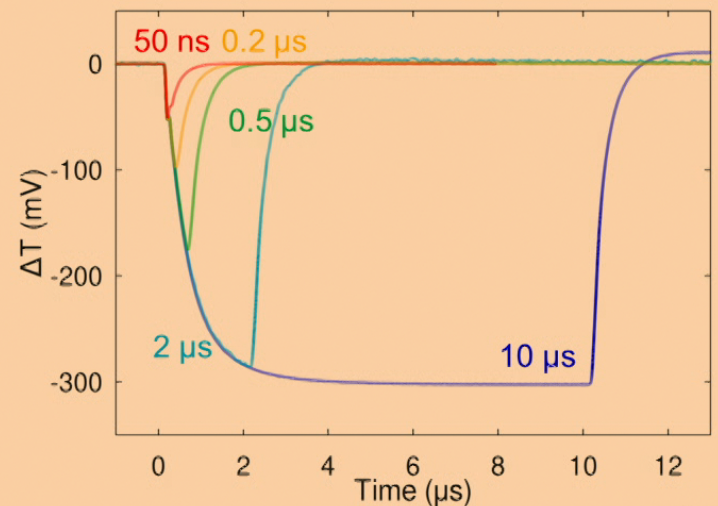
Outline

1. What are atomic limits on temporal resolution?

- Can detect sub-50 ns pulses at low Ω_p
- Influenced by $\sim\mu\text{s}$ transit time & fields (ions, collisions)
- $240 \text{ nV cm}^{-1} \text{ Hz}^{-1/2}$ sensitivity aided by matched filtering
- Timing resolution sub-30 ns for radar applications



S. Bohaichuk, arXiv:2203.01733 (2022).



S. Bohaichuk

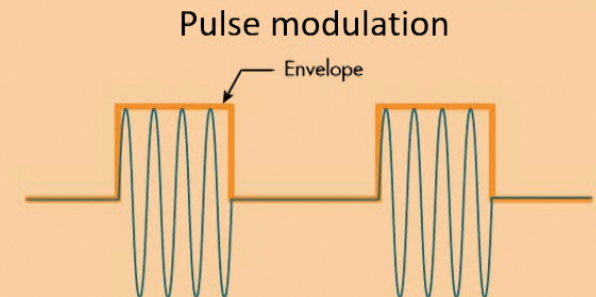
Quantum Valley
Ideas Lab

23

Outline

1. What are atomic limits on temporal resolution?

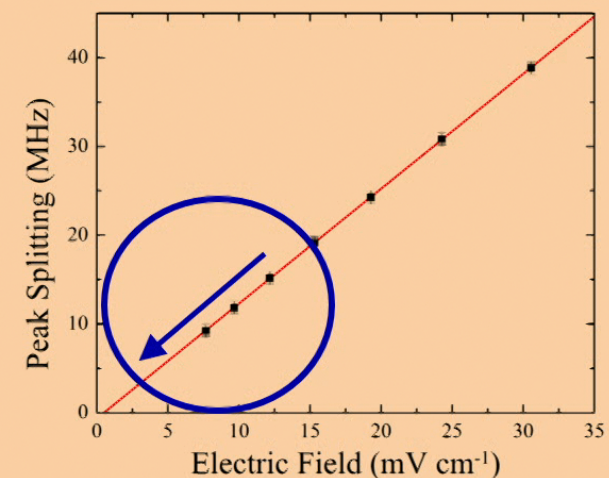
- Can detect sub-50 ns pulses at low Ω_p
- Influenced by $\sim \mu\text{s}$ transit time & fields (ions, collisions)
- $240 \text{ nV cm}^{-1} \text{ Hz}^{-1/2}$ sensitivity aided by matched filtering
- Timing resolution sub-30 ns for radar applications



S. Bohaichuk, arXiv:2203.01733 (2022).

2. How can we improve sensitivity?

- Weakest field detectable in shortest time
- Extension of Autler-Townes regime to lower fields

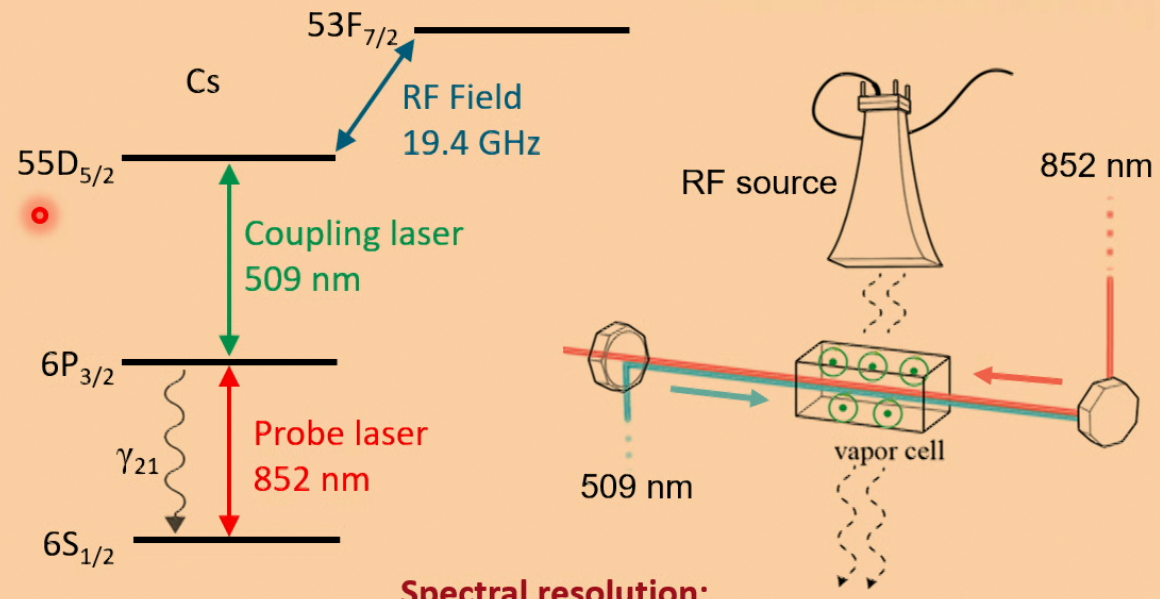
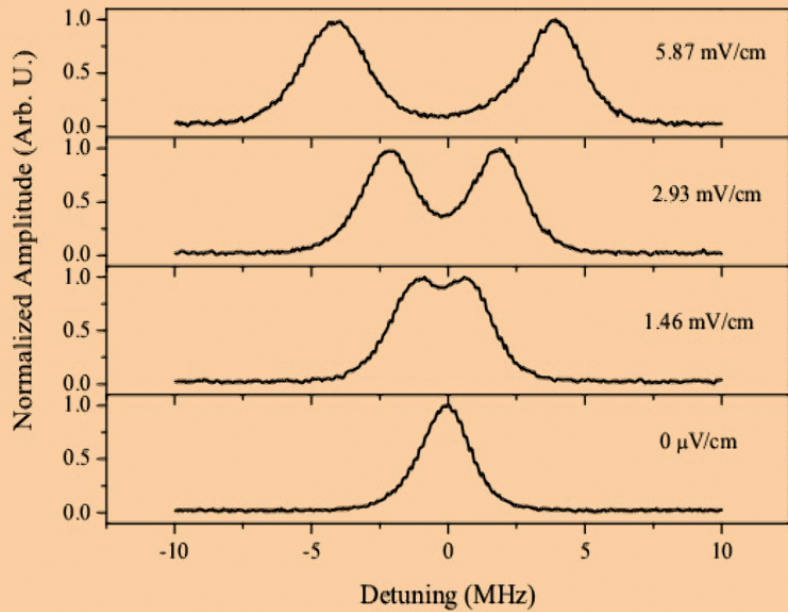


S. Bohaichuk

Quantum Valley
Ideas Lab

23

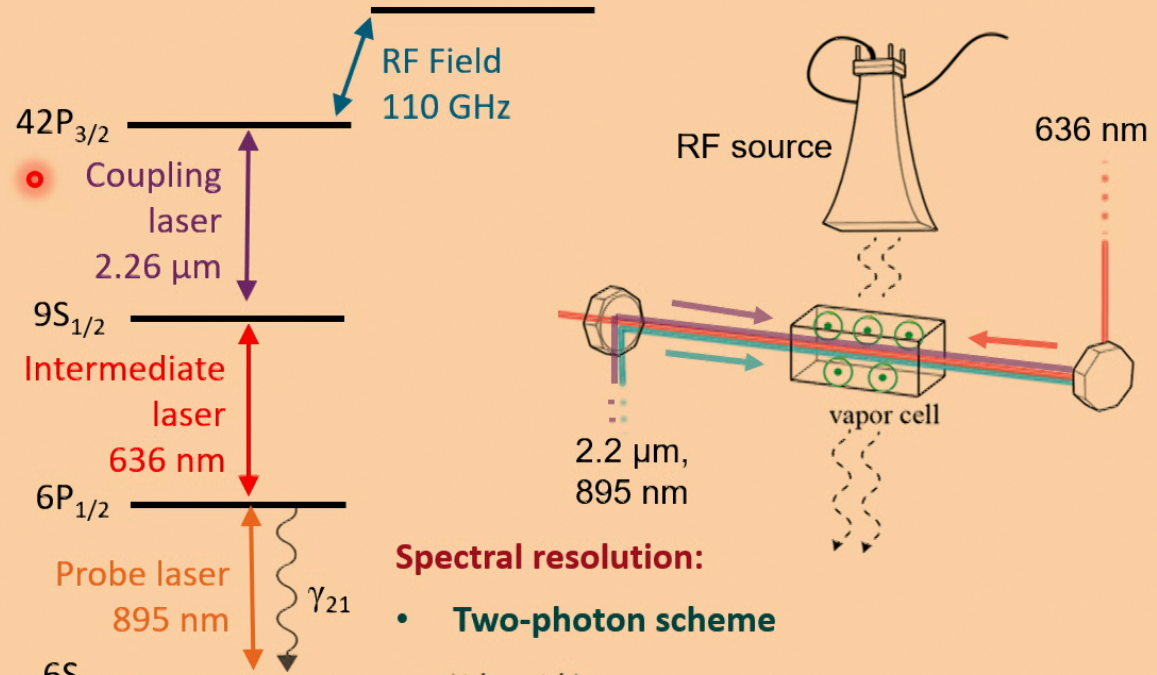
2-Photon Autler-Townes Limit



Spectral resolution:

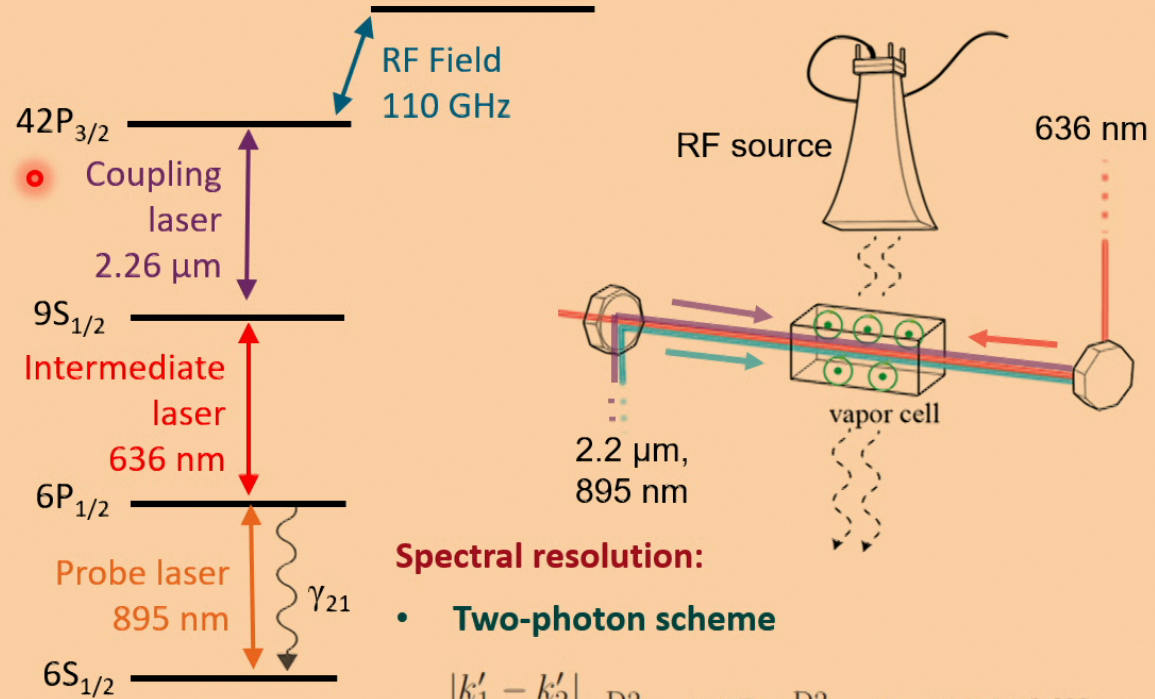
- Extent of Autler-Townes regime set by EIT linewidth
- Spectral resolution of 2-photon scheme limited by residual Doppler shifts:
$$\frac{|k'_1 - k'_2|}{k'_1} \gamma_{21}^{D2} = 0.671 \gamma_{21}^{D2} = 2\pi \times 3.50 \text{ MHz}$$

Enhanced 3-photon Scheme



- Typical 2-photon conditions are limited to several MHz linewidth

Enhanced 3-photon Scheme



- Typical 2-photon conditions are limited to several MHz linewidth
- Lower 3-photon wavevector mismatch gives <200 kHz linewidth

S. Bohaichuk

Quantum Valley
Ideas Lab

Spectral resolution:

- Two-photon scheme**

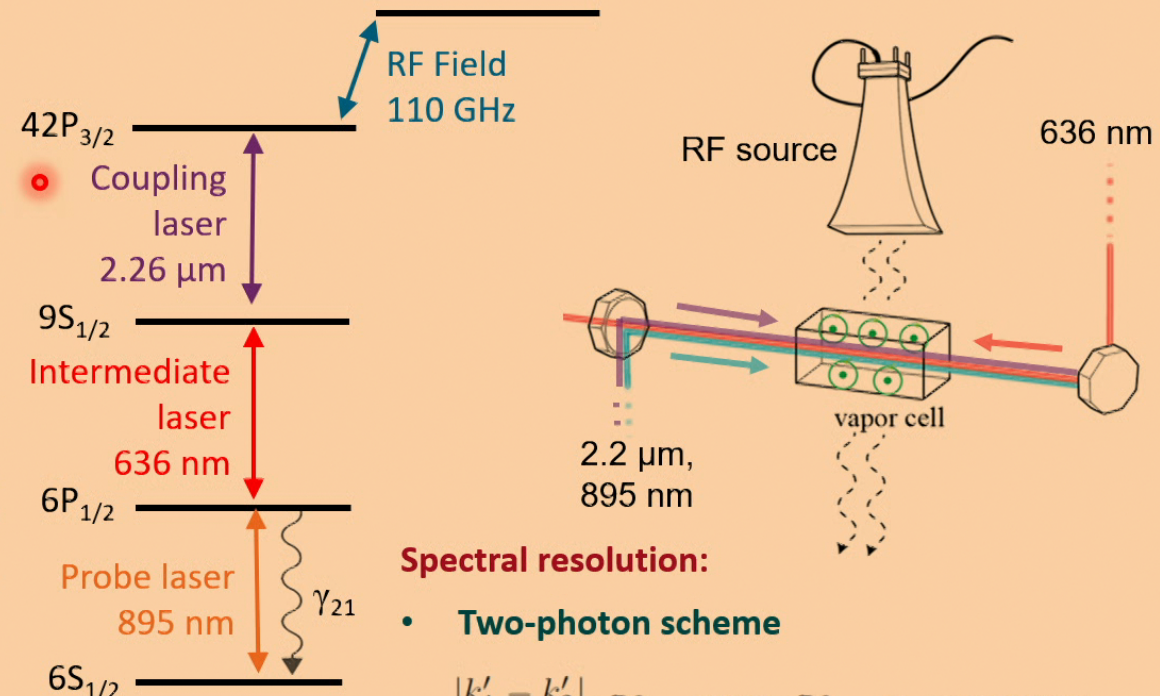
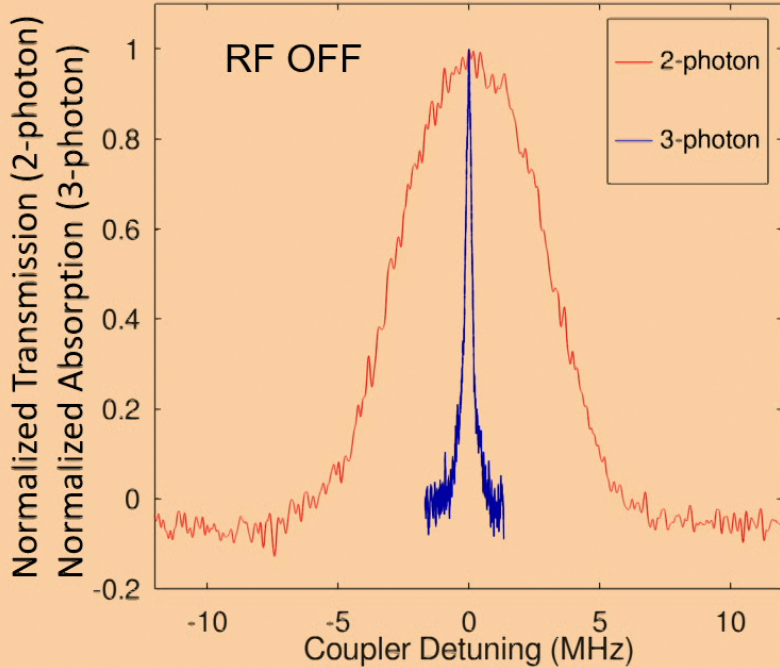
$$\frac{|k'_1 - k'_2|}{k'_1} \gamma_{21}^{D2} = 0.671 \gamma_{21}^{D2} = 2\pi \times 3.50 \text{ MHz}$$

- Three-photon scheme**

$$\frac{|k_2 - k_1 - k_3|}{k_1} \gamma_{21}^{D1} = 0.0048 \gamma_{21}^{D1} = 2\pi \times 21.9 \text{ kHz}$$

25

Enhanced 3-photon Scheme



- Typical 2-photon conditions are limited to several MHz linewidth
- Lower 3-photon wavevector mismatch gives <200 kHz linewidth

S. Bohaichuk

Quantum Valley
Ideas Lab

Spectral resolution:

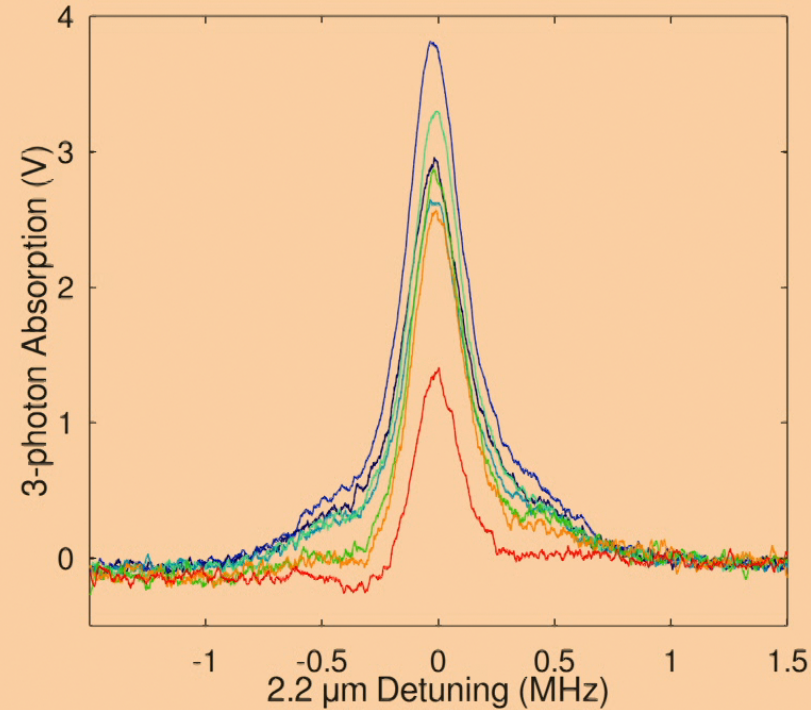
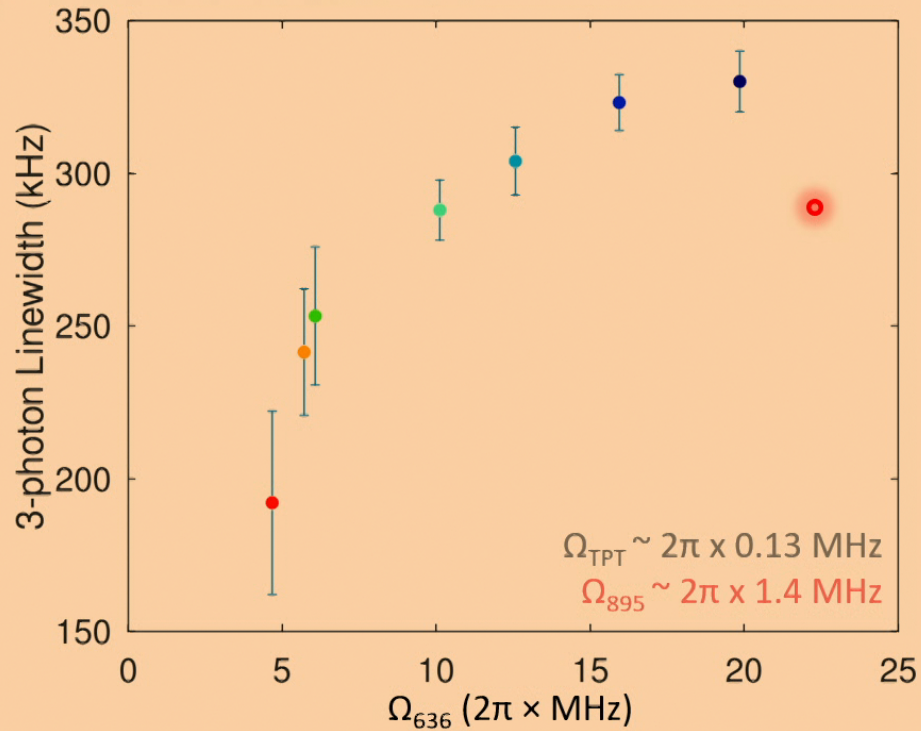
Two-photon scheme

$$\frac{|k'_1 - k'_2|}{k'_1} \gamma_{21}^{D2} = 0.671 \gamma_{21}^{D2} = 2\pi \times 3.50 \text{ MHz}$$

Three-photon scheme

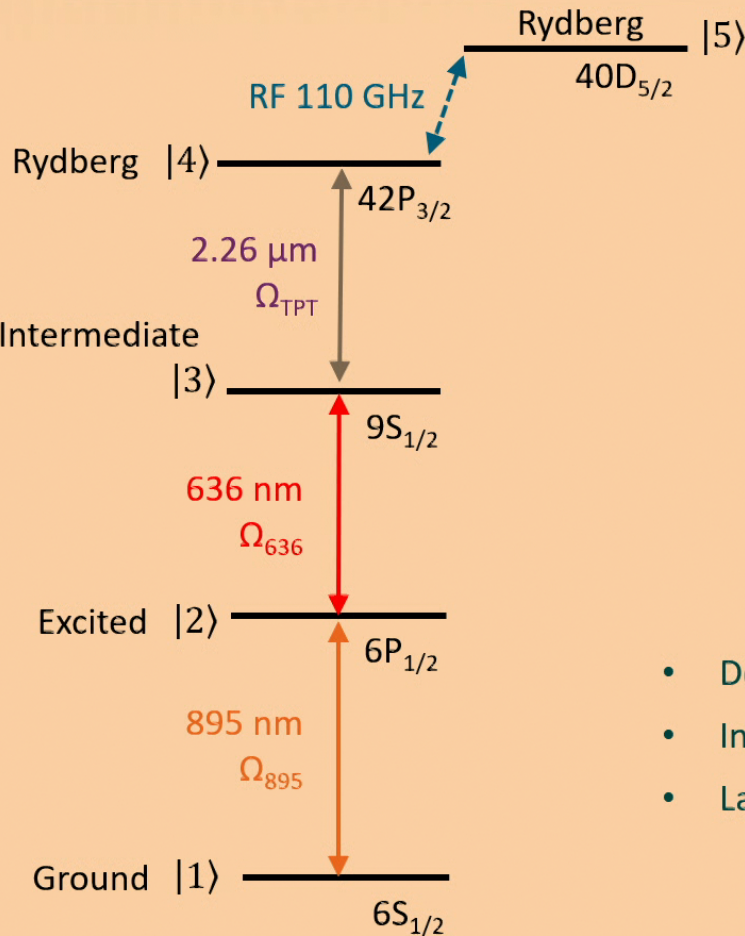
$$\frac{|k_2 - k_1 - k_3|}{k_1} \gamma_{21}^{D1} = 0.0048 \gamma_{21}^{D1} = 2\pi \times 21.9 \text{ kHz}$$

Experimental 3-Photon Linewidth



- Narrowest linewidth <200 kHz at low red coupling Rabi frequencies

Density Matrix Model



Typical Rabi Frequencies:

$$\Omega_{\text{TPT}} \sim 2\pi \times 0.13 - 0.4 \text{ MHz}$$

$$\Omega_{636} \sim 2\pi \times 0.5 - 20 \text{ MHz}$$

$$\Omega_{895} \sim 2\pi \times 0.3 - 2.4 \text{ MHz}$$

Decays:

$$\begin{aligned}\Gamma_{21} &= 2\pi \times 4.52 \text{ MHz} + \Gamma_{\text{tt}} \\ \Gamma_{32} &= 2\pi \times 200 \text{ kHz} \\ \Gamma_{31} &= \Gamma_{\text{tt}} \\ \Gamma_{41} &= 2\pi \times 20 \text{ kHz} + \Gamma_{\text{tt}} \\ \Gamma_{\text{tt}} \text{ (transit time)} &\sim 2\pi \times 80 \text{ kHz}\end{aligned}$$

Laser Linewidths:

$$\left. \begin{aligned}\Gamma_{895} &= 2\pi \times 20 \text{ kHz} \\ \Gamma_{636} &= 2\pi \times 50 \text{ kHz} \\ \Gamma_{\text{TPT}} &= 2\pi \times 50 \text{ kHz}\end{aligned}\right\}$$

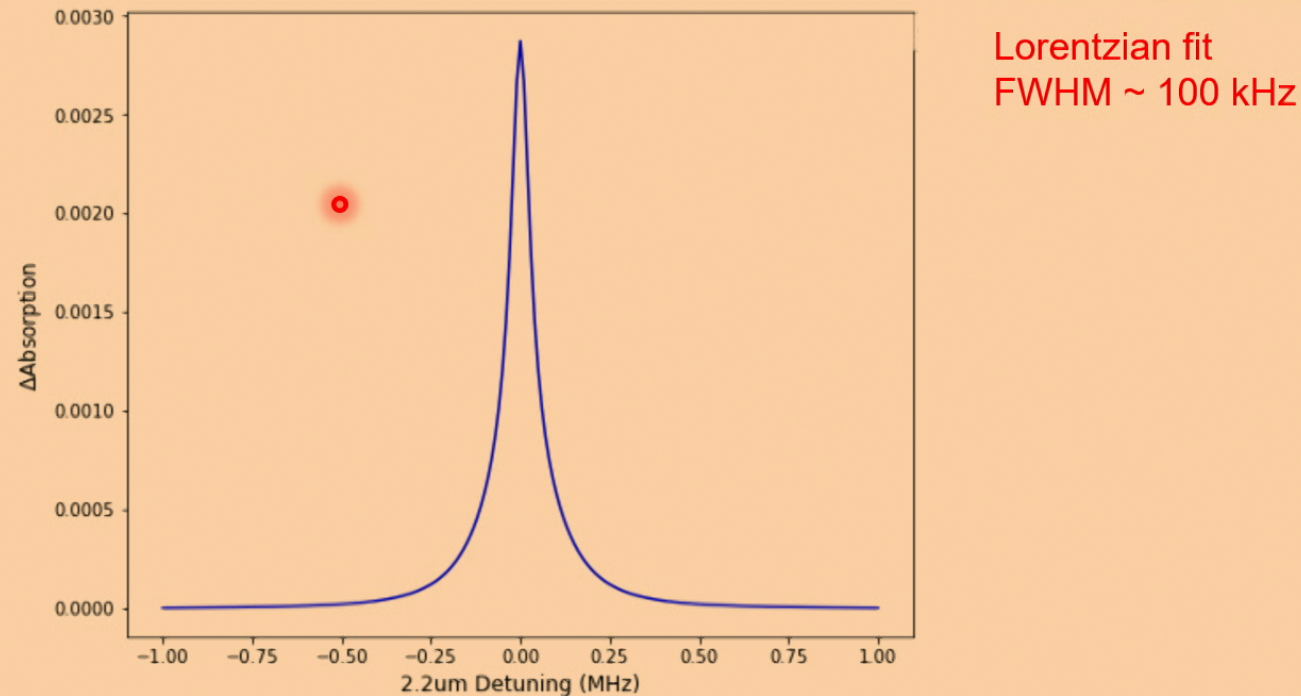
Dephasings:

$$\left. \begin{aligned}\Gamma_{11} &= \Gamma_{895} \\ \Gamma_{22} &= \Gamma_{895} + \Gamma_{636} \\ \Gamma_{33} &= \Gamma_{636} + \Gamma_{\text{TPT}} \\ \Gamma_{44} &= \Gamma_{\text{TPT}}\end{aligned}\right.$$

- Density matrix model used to estimate theoretical narrowest linewidth
- Includes known decay rates between the states & transit time broadening
- Laser linewidth estimates included as dephasing terms

Simulated Linewidth

$$\begin{aligned}\Omega_{\text{TPT}} &\sim 2\pi \times 0.13 \text{ MHz} \\ \Omega_{636} &\sim 2\pi \times 10 \text{ MHz} \\ \Omega_{895} &\sim 2\pi \times 1.4 \text{ MHz}\end{aligned}$$



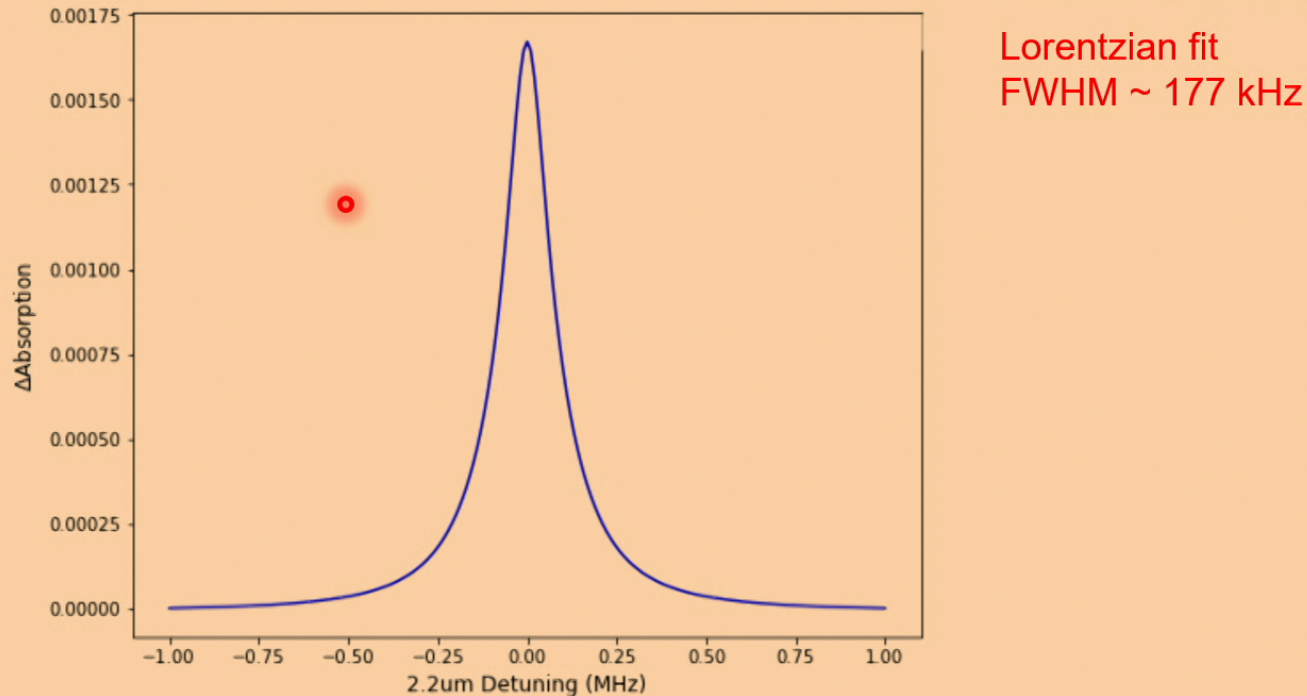
- No laser linewidths or transit time broadening included

Simulated Linewidth

$$\begin{aligned}\Omega_{\text{TPT}} &\sim 2\pi \times 0.13 \text{ MHz} \\ \Omega_{636} &\sim 2\pi \times 10 \text{ MHz} \\ \Omega_{895} &\sim 2\pi \times 1.4 \text{ MHz}\end{aligned}$$

Linewidths:

$$\begin{aligned}\Gamma_{895} &= 2\pi \times 20 \text{ kHz} \\ \Gamma_{636} &= 2\pi \times 50 \text{ kHz} \\ \Gamma_{\text{TPT}} &= 2\pi \times 50 \text{ kHz}\end{aligned}$$



Lorentzian fit
FWHM ~ 177 kHz

- No transit time broadening included
- Laser linewidths are included as dephasing, resulting in a 77 kHz increase in linewidth

Simulated Linewidth

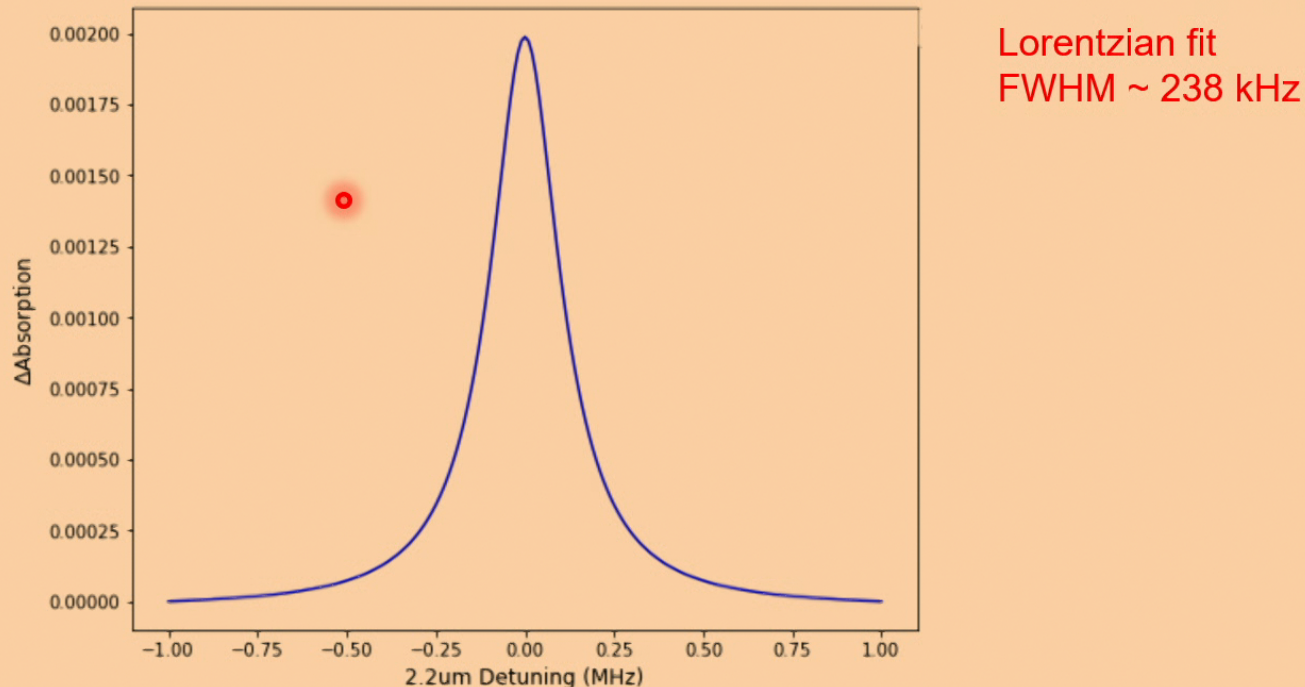
$$\begin{aligned}\Omega_{\text{TPT}} &\sim 2\pi \times 0.13 \text{ MHz} \\ \Omega_{636} &\sim 2\pi \times 10 \text{ MHz} \\ \Omega_{895} &\sim 2\pi \times 1.4 \text{ MHz}\end{aligned}$$

Linewidths:

$$\begin{aligned}\Gamma_{895} &= 2\pi \times 20 \text{ kHz} \\ \Gamma_{636} &= 2\pi \times 50 \text{ kHz} \\ \Gamma_{\text{TPT}} &= 2\pi \times 50 \text{ kHz}\end{aligned}$$

Transit time:

$$\Gamma_{\text{tt}} \sim 2\pi \times 80 \text{ kHz}$$



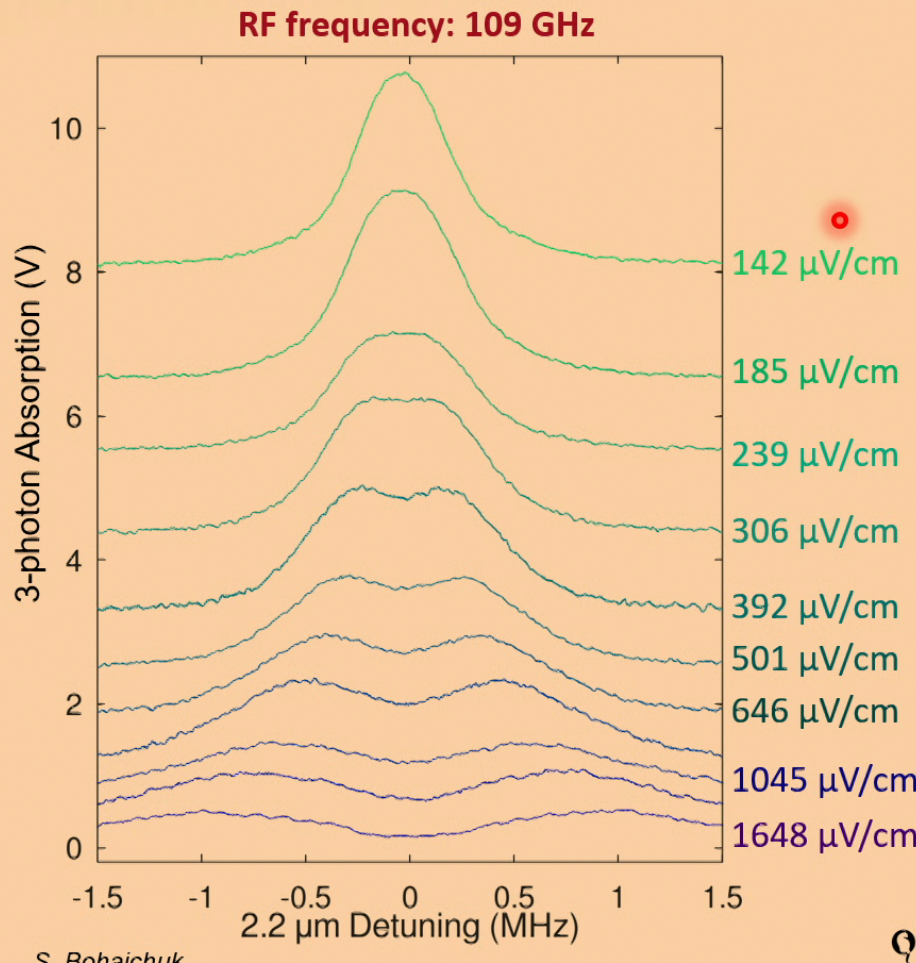
- Transit time broadening included, resulting in a 61 kHz increase in linewidth
- Laser linewidths are included as dephasing
- At these Rabi frequencies expect around 250 kHz, consistent with experiment

S. Bohaichuk

Quantum Valley
Ideas Lab

30

Autler-Townes Regime Extension



- Smallest RF field strength detected in self-calibrated Autler-Townes regime using 3-photon <math><300 \mu\text{V}/\text{cm}</math>
- Measured with a linewidth (FWHM) $\sim 315 \text{ kHz}$

S. Bohaichuk

Quantum Valley
Ideas Lab

31

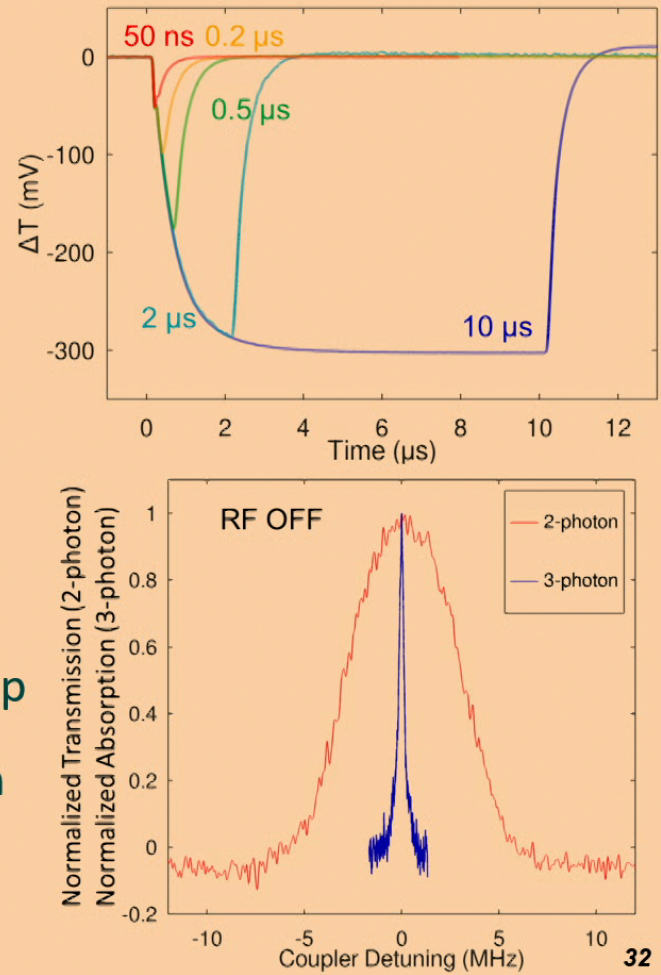
Conclusion

1. What are atomic limits on temporal resolution?

- Can detect sub-50 ns pulses at low Ω_p
- Influenced by $\sim\mu\text{s}$ transit time & fields (ions, collisions)
- $240 \text{ nV cm}^{-1} \text{ Hz}^{-1/2}$ sensitivity aided by matched filtering
- Timing resolution sub-30 ns for radar applications

2. How can we improve sensitivity?

- Reduction in linewidth to $< 200 \text{ kHz}$ with 3-photon setup
- Extension of Autler-Townes to lower fields $< 300 \mu\text{V/cm}$



S. Bohaichuk

Quantum Valley
Ideas Lab

Thanks



Stephanie Bohaichuk
James P. Shaffer
Don Booth
Fabian Ripka
Matthias Schmidt
Chang Liu
Kent Nickerson
Harry Tai
Harald Kubler
Jennifer Erskine





Opportunities and Limitations for Rydberg Sensors

Paul Kunz
Quantum Science Branch
Army Research Lab (ARL)

CATMIN, July 15, 2022